ALMA MATER STUDIORUM - UNIVERSITÀ DI BOLOGNA
CAMPUS DI CESENA

DIPARTIMENTO DI

INGEGNERIA DELL'ENERGIA ELETTRICA
E DELL'INFORMAZIONE *"GUGLIELMO MARCONI"*

CORSO DI LAUREA IN

INGEGNERIA ELETTRONICA PER L'ENERGIA E L'INFORMAZIONE

Mobile Radio Channel Measurements for Air-to-Ground and non-conventional Future Applications

Elaborato in
Propagazione Elettromagnetica Libera

Relatore:
Prof. Ing. Vittorio Degli Esposti

Presentato da:
Roberto Cirillo

Correlatore:
Prof. Ing. Enrico Maria Vitucci

Anno accademico **2018/2019**
Sessione **II**

TABLE OF CONTENTS

INTRODUCTION

Today, the word “progress” is a sort of buzzword used for all those situations dealing with technology and engineering. “Progress” is the Google Home, a 4K television, a new computer or even those odd cameras on the new iPhone 11.

But to me, progress means something which can really change our point of view, something new, something helpful.

Nowadays the rapid increase of mobile data is creating unprecedented challenges for wireless service providers to overcome a global bandwidth shortage. In fact, as today’s cellular companies try to deliver high quality, low latency and multimedia applications, they are limited to a carrier frequency spectrum ranging between 700 MHz and 6 GHz, which is now basically saturated.

We need new spectrum and that is also related to the main purpose of this thesis.

We focused our attention on Millimeter Wave and Ultra-Wide Band signals which are likely to be fundamental parts of future 5^{th} generation (5G) cellular networks.

We have operated in a factory scenario, a rich-of-scattering environment where propagation of signal at high frequency is continuously affected and many Multi-Path Component arise from reflections and diffractions.

The aim was studying the received signal from different points of view and angulations, to obtain the Power Angle Delay Profile, which is a crucial step to determine the performance of future beamforming transmission techniques in this challenging environment. The results are interesting.

UWB signals confirmed their enormous potential in indoor positioning, and the polar plots suggest an easy distribution of power.

Here is a list divided by chapters of the topics covered in this work:

- Chapter one. A brief introduction of UAVs, classification, regulation and their role in communication applications and beyond.
- Chapter two. Definition of an Air-to-Ground Channel, characteristics and modelling for different scenarios.
- Chapter three. Overview of Ultra-Wide Band signals and advantages, introduction to Time Domain equipment.
- Chapter four. Overview of Millimeter Wave signals and advantages, introduction to SAF Tehnika equipment.
- Chapter five. Measurement Campaign in factory environment, description of the experiments, PAPs and Impulsive response.
- Chapter six. Measurement Campaign in Urban environment, only plan of measurement, results will be available soon.

CHAPTER 1

UAV AND THEIR USE FOR TELECOMMUNICATION AND SENSING

1.1 UAV: Description and classification.

1.1.1 What is a UAV? Classification and characteristics.

The acronym UAV stands for Unmanned Aerial Vehicles, that is aircrafts without a human pilot aboard. They are also commonly known as drones or Remotely Piloted Aircrafts (RPA).

Depending on the application and goals, there is a type of UAV which best meets the requirements imposed by the nature of environment, the aim, or the federal regulations. In general, UAVs can be categorized through two different characteristics: their flying altitude and their capabilities (see *Fig. 1.a*)

Based on the altitude, we can distinguish two types of drones:

- The High-Altitude Platform (HAP), [1] which are characterized by a long endurance (days or months), wide coverage and they are typically quasi-stationary. Their altitude is usually above 17 km.
- The Low-Altitude Platform (LAP), [2] on the other hand, do not have a long endurance (typically they fly up to several hours), but they can be deployed more rapidly, and they are in general more flexible (they can easily be recharged or replaced). They are cost-effective, and their altitude is usually under 2 km.

Based on the capability, UAVs can be categorized also into:

- Fixed-wing UAVs, which are essentially like small aircrafts. They have more weights, higher speed, and they need to move forward in order to remain aloft

(they cannot hover). Thanks to their stability, fixed-wings UAVs can carry high payload and fly for several hours.

- Rotary-wing UAVs, among them the well-known "quadcopter", can hover and remain stationary over an area (which is very useful for a lot of applications). Compared to the fixed-wings ones, however, they have plenty of limits due to their nature, for instance, their low speed and their energy limitations, which causes a shorter duration of flight (less than 1 hour for typical drones).

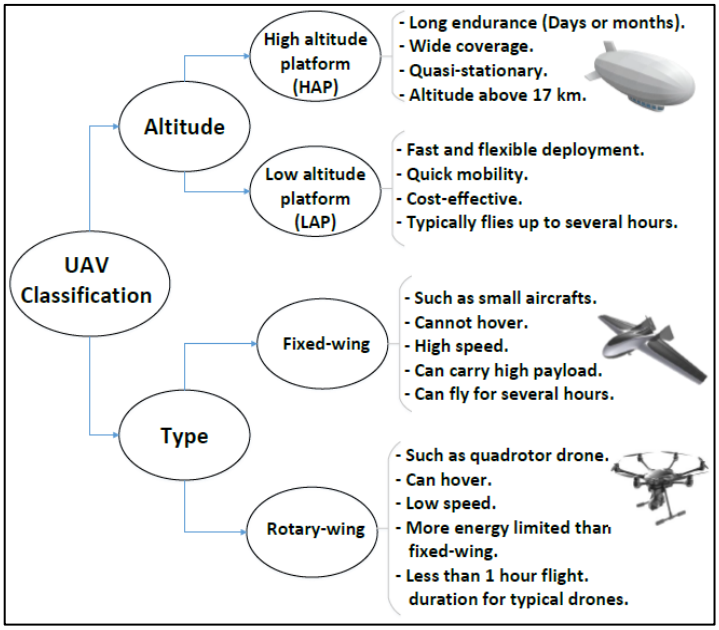

Figure 1.a UAV Classification depending on Altitude and Type

1.2 UAVs use and regulation.

1.2.1 Why do we need a Regulation?

In recent years, the use of unmanned aircraft vehicles (UAVs) has grown rapidly. These vehicles are being used worldwide for an ever-growing number of applications. Example, applications including cargo transport, public safety, search and rescue, agriculture, scientific and industrial surveys, and of course for military use [3]. According to [4] the number of UAVs in the USA will reach 230 000 in 2035, and for some scientists even more.

Hence, due to this rapid growth, numerous organizations are working to ensure the safe and reliable integration of them into the airspace worldwide. We need a safe regulation through which all the UAV-assisted operations can be done easily and without any risks.

Among this organizations, the ENAC (Ente Nazionale per l'Aviazione Civile) is the national civil aviation authority of Italy and it deals with the technical regulation, certification, and supervision of the aviation sector.

As regards drones, ENAC divides rules and articles into three main sections:

- Aircraft with operating take-off mass of less than 25 Kg;
- Aircraft with operating take-off mass of more than or equal to 25 Kg;
- General rules of circulation and use of airspace.

1.2.2 Operation with a specific take-off mass.

With operation with take-off mass less than 25 Kg the operator must have a Remotely Piloted Aircraft System (RPAS) Pilot Certificate, issued by a recognized RPAS training centre.

There are two types of operations we can do with a "light" drone:

- Non-Critical: Visual Line Of Sight (VLOS) operations which do not overfly congested area, gathering of persons, urban areas, or critical infrastructures. In this part drones with take-off mass less than 2 Kg are included.

  Before commencing, the operator shall provide ENAC with the declaration of compliance to the applicable sections of the regulation.
- Critical: all the operations that do not respect, even partially, the conditions of Non-Critical operation. Before commencing, the operator shall apply for and obtain the authorization by ENAC, unless the operation does not fall into standard scenarios published by ENAC.

With operation with take-off mass more than 25 Kg the operator must have a RPAS pilot Licence issued by ENAC. This type of drone shall be registered by ENAC in the RPAS register, by assigning dedicated registration marks.

RPAS are approved to fly by holding a Permit to Fly (maximum validity period of three years) which shall be issued by ENAC upon successful completion of the review necessary to verify that the proposed operations can be carried out with an adequate level of safety.

1.2.4 General rules of circulation and use of airspace.

The RPAS shall be identified by a plate installed on the RPA showing the identification of the system and of the operator (same on the remote ground pilot station) and equipped with an Electronic Identification Device.

Then, the regulation provides some general rules depending on the type of operation:

- Visual Line Of Sight (VLOS) operations are permitted in daylight, up to maximum height of 150m, within maximum horizontal distance of 500m.
- Extended VLOS (EVLOS) operation permitted according to the limitations required for VLOS operations.
- Beyond VLOS (BVLOS) operation, when distances do not allow the remote pilot to continuously remain in direct visual contact with the RPA. These operations require systems and procedures to maintain separations and avoid collision.

1.3 UAVs for communication applications.

1.3.1 UAV-aided ubiquitous coverage and relaying.

UAVs will probably be deployed to assist the existing communication infrastructure, if any, in providing seamless wireless coverage within the serving area. Two example scenarios (*Fig. 1.b*) are rapid service recovery after partial or complete infrastructure damage due to natural disaster, and base station offloading in extremely crowded areas (for instance, a stadium during an important football match). This is one key scenario addressed by fifth generation (5G) wireless systems. [5]

In the case of UAV-aided relaying, UAVs are deployed to provide wireless connectivity between two or more distant users or user groups without reliable direct communication links. [6] For example, (*Fig 1.b*) this could happen between the frontline and the command centre for emergency responses.

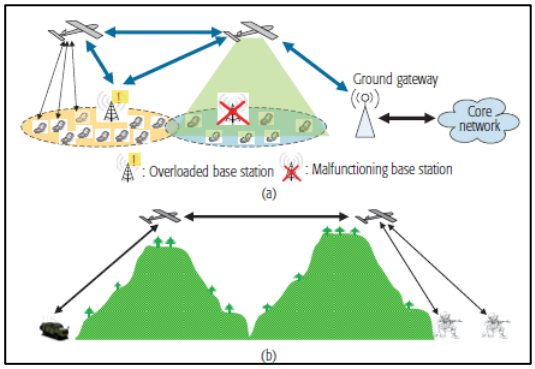

Figure 1.b UAV-aided ubiquitous coverage and UAV—aided relaying

1.3.3 UAVs for 5G communication.

5G, which stands for "5th generation", is the latest generation of cellular mobile communication. 5G will be revolutionary thanks to the unbelievable performances, which would have not been possible with the previous standards of wireless communication.

This new technology targets high data rate, reduced latency, energy saving, cost reduction, higher system capacity and massive device connectivity, thanks to the development of new wireless technologies, such as device-to-device (D2D) communications, ultra-dense small cell networks, and millimetre wave (mmWave) communications (especially combined with MIMO techniques), which are known as the nexus of 5G cellular systems.

However, despite their invaluable benefits, those solutions have strong limitations of their own: a lack of an optimal frequency planning, open problems concerning backhaul, interference and high reliance on Line of Sight (LoS) communication. Hence, UAV-carried flying base stations represent an inevitable complement for such a heterogeneous 5G environment. For instance:

- LAP-UAVs can provide rapid, and cost-effective on-the-fly communications, instead of deploying ultra-dense small cell network in rural and geographically constrained environments.
- HAP-UAVs can provide more long-term sustainable solutions for coverage in rural environments.
- UAVs equipped with mmWave capabilities can naturally establish LoS connections to ground users (which significantly reduces propagation loss). This can be an attractive solution to provide high capacity wireless transmission, while leveraging the advantages of both UAVs and mmWave links. Moreover, combining these types of UAV with potentially massive Multiple Input Multiple Output (MIMO) techniques, can create a whole new sort of dynamic cellular network that can provide high capacity wireless services.

- Device-to-Device (D2D) and Vehicle-to-Vehicle (V2V) communications could be much more efficient. Firstly, drones can mitigate interference by reducing the number of required transmission links between ground devices. Secondly, mobile drones can introduce transmit diversity opportunities and boosting reliability and connectivity in D2D and V2V terrestrial networks, as shown in figure 1.c.

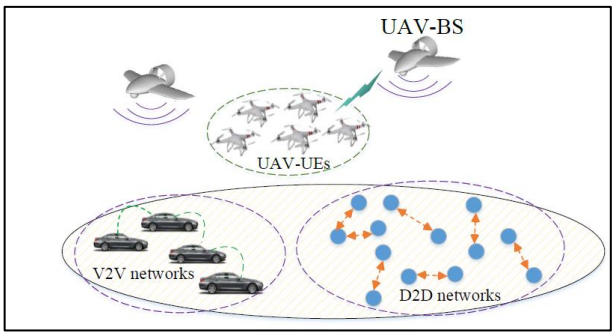

Figure 1.c Device-To-Device and Vehicle-to-Vehicle Communication example

1.3.4 UAVs for IoT communication.

In an IoT (Internet of Things) environment energy efficiency, ultra-low latency, reliability, and high-speed uplink communications become extremely important. In this regard, the use of mobile UAV can be deployed as flying base stations to provide reliable and energy-efficient uplink IoT communications. In fact, due to their nature, drones can be effectively deployed to reduce the shadowing and blockage effects. As a result, the communications channel between IoT devices and UAVs is significantly improved. Moreover, UAVs can help connecting IoT devices to the network using a minimum transmit power, in order to save energy.

1.4 UAVs for sensing applications.

1.4.1 UAVs as Flying BS for Public Safety Scenarios.

During wide-scale natural disasters and unexpected events, the existing terrestrial communication networks can be damaged or even destroyed, thus becoming significantly overloaded. In such scenarios there is a vital need for public safety communications between first responders and victims for search and rescue operations. A robust, fast and capable emergency communication is needed not only to improve connectivity, but also to save lives.

As shown in *Fig. 1.d*, the use of UAV-based aerial networks [7] is a promising solution to enable fast, flexible and reliable wireless communications in public safety scenarios. Drones can easily fly and dynamically change their positions to provide on-demand communications to ground users in emergency situations. For instance, UAVs can be deployed as mobile aerial base stations to deliver broadband connectivity and to provide full coverage to a given area within a minimum possible time.

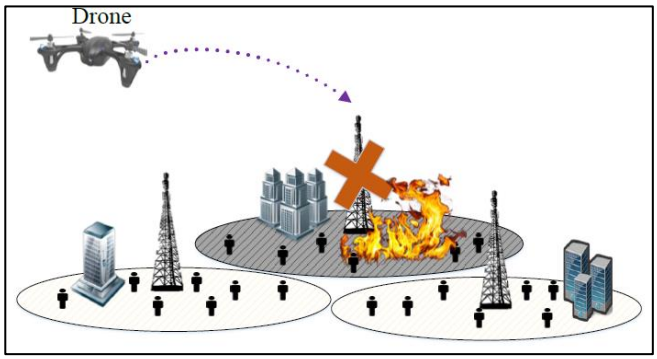

Figure 1.d UAV-based aerial networks example

1.4.2 Detection of unauthorized drones for Public Security.

The increase in the number of amateur drones demands more stringent regulations on their allowed route, mass, and load. However, these regulations may be violated accidentally or deliberately. So, drones whose only purpose had always been aiding people, could be used as a harmful weapon. For instance, spying UAVs, transfer of dangerous payloads, terroristic attacks.

The technologies to detect, track, and disarm possible aerial threats are therefore in prompt demand. To this end, ubiquitous cellular networks, and especially 5G infrastructures based on the use of millimetre-wave radio modules, may be efficiently leveraged to offer suspicious drone detection.

Many researches have been done about this issue, the most attractive one accurately demonstrates how the utilizations of 5G mmWave (with high-gain antenna) BSs (Base Stations) as emitters to realize a passive radar scheme. [8].

Finally, another important sensing application with drones is the precision agriculture where UAVs are despatched to disseminate (or collect) delay-tolerant information to (from) a large number of distributed wireless devices. (*Fig 1.e*)

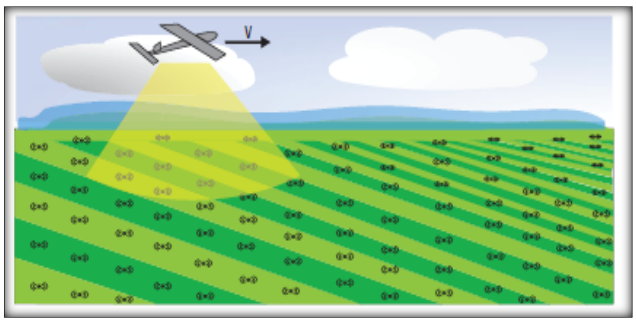

Figure 1.e UAV for precision agriculture applications.

CHAPTER 2

AIR TO GROUND CHANNEL CHARACTERIZATION

2.1 The Air-to-Ground Channel: Basic Characteristics.

2.1.1 Brief Introduction and Literature.

Nowadays, Unmanned Aircraft Systems (UAS) are being used more frequently and more widely. In fact, a recent report by the United States Department of Transportation [4] predicts that by 2035, there will be over 230,000 UAS aloft in the United States alone. So, the drones are supposed to become more and more ubiquitous and ensuring safety will become necessary.

Surely, a required element in ensuring UAS safety is a reliable communication link (A2G Channel), which must account for the unique operating conditions and for all the constraints that they will lead to.

A moderate body of literature exists for the Air-to-Ground Channel (A2G Channel see [9] for a complete overview), but the number of papers in the literature about this particular topic is far smaller than the number on other types of channels such as cellular radio. That is why in the last few years, more and more researches are addressed to the characterization of the A2G Channel with particular interest in communication with drones.

2.1.2 Description and characteristics of A2G Channel.

We define this channel as that used for electromagnetic signalling between a ground station (GS) and a human-made flying platform aloft in the atmosphere. As already said, there are a lot of similar studies for similar applications (e.g. cellular radio or the satellite to earth communication), but in this case we need a

reliable model which include all the constraints and characteristics of a communication between a fixed GS and a dynamic UAV in the air.

The main difference between a satellite to earth communication and an A2G Channel for drones is the environment of work. The A2G Channel will often, but not always, contain a line-of-sight (LOS) component. Shadowing may occur due to obstacles, such as buildings, terrain, trees, or even from the aircraft itself (a phenomenon called "airframe shadowing"). Furthermore, notable differences in the satellite case can include higher elevation angles, different relative velocities, and propagation effects for the atmospheric layers.

There are also some assumptions we must consider studying the A2G Channel, for instance, the fact that the UAV is supposed to be within "radio line of sight" (RLOS) of the GS, since attenuation increases very rapidly beyond this distance due to earth curvature [10], making link closure essentially impractical beyond RLOS distance.

Another important aspect of the A2G Channel is the" Multipath components" (MPCs). This occur primarily from surface-based obstacles and their number and relative strength depends on the environment surrounding the GS and in general within the volume between the GS and aircraft.

2.1.4 The Networking architecture.

As shown in *Fig. 2.a,* this is the generic networking architecture of wireless communications with UAVs, which consists of two basic types of communication links: the "Control and Non-Payload Communication" (CNPC) link and the "Data link" (for more details see [6])

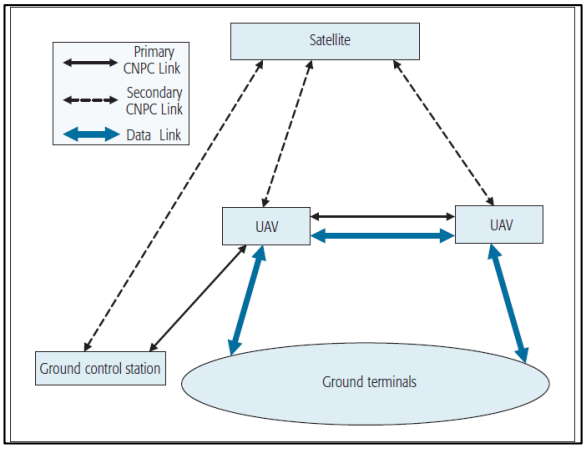

Figure 2.a Generic Networking Architecture of Communication with UAVs.

- The CNPC Links are essential to ensure the safe operation of all UAV systems. The main CNPC information flow can be broadly categorized into three types: command and control from Ground Control Station (GCS) to UAVs, aircraft status report from UAV to ground and sense-and-avoid information among UAVs. Finally, due to the critical functions, CNPC links should in general operate in protected spectrum.
- The Data Link, instead, aim to support mission-related communications for the ground terminals, which, depending on the application scenarios, may include terrestrial base stations (BSs), mobile terminals, gateway nodes, sensors and so on. The Data Link maintained by the UAVs need to support the following communication modes: Direct mobile-UAV communication as for BS offloading or during compete BS malfunction and wireless backhauling (UAV-gateway or UAV-UAV).

2.1.5 Spectral allocations.

Regarding the spectral allocations for UAVs, these have been established in the L-band (1-2 GHz) and in the C-band (4-8 GHz), but since many other systems (aviation and otherwise) operate in these bands, the actual available spectrum is limited: there is approximately 17 MHz (960-977 MHz) at the L-band and 61

MHz (5.03-5.091 GHz) at the C-band presently allocated for UAS CNPC. This limited spectrum presents significant challenges to the design of a high-capacity CNPC network.

Another important aspect to consider is the difference between the propagation conditions using one band or the other one. For instance, free-space path loss is approximately 14 dB larger in the C-band. Furthermore, the factor of five wavelength difference also means that reflecting surfaces are considerably smoother at the L-band. This has implications for the strength of MPCs, which can produce a distortion of the signals.

2.2 The Air-to-Ground Channel: Modeling Overview.

2.2.1 Modeling Introduction.

In the analysis of the A2G Channel, one fundamental aspect is the mathematic model we are referring to.

For instance, if we are in a free of obstacles environment, with no surface reflections (or reasonably very weak) and without considering very long distance, simple attenuation models suffice, which means that the “free-space model” can be used. If distance increases, then considering the curvature of the earth may be an optimal approximation (the “Curved-Earth two-ray model”, CE2R).

On the other hand, depending on the scenario, we can have different situations, different types and/or number of obstacles (buildings, trees, bushes...) and that is why a more accurate model is needed.

2.2.2 Principal Model types and Classes.

As already said, there is not a favourite model, but it critically depends on the scenario we are dealing with (see [11]).

There are both deterministic and stochastic models which can be used (also in a combination of them). Here is a list of the most used ones.

- "Two-ray model", which consists of one LOS component and one surface reflection. That is the simplest way to approximate the A2G Channel and it can be very useful with narrowband signals, but it is clearly an approximation and becomes inaccurate when additional MPCs are present. Still, it can be improved with scale fading parameters (for instance the "Ricean factor) or introducing random obstacles.
- "Stored CIRs model". CIR stands for time-varying Channel Impulse Response and the model can collect all these stored samples and put them into a simulation. Such samples represent real channel conditions for the given measurement setting.
- "High-frequency approximation" (geometry-based e.g., ray optics) include ray-tracing and ray launching approaches and assume all objects in the environment have dimensions large with respect to wavelength. These models also require a large environment database, so computation time is large and can be modified with statistical parameters to improve accuracy. For instance the Geometry-Based Stochastic Channel Model (GBSCM), which employ ray tracing with stochastically distributed objects.
- "Stochastic models", which traditionally take the form of Tapped-Delay Lines (TDLs) and assume wide-sense stationarity. These models are in general more efficient in implementation and can be improved with deterministic parameters (CIR features or statistical distribution for MPC delays).

2.2.3 The Curved-Earth Two Ray Model (CE2R) and the Path Loss.

The simple "two-ray model" could be termed as the "canonical model" for the A2GChannel, that is because there are plenty of conditions where MPCs are typically weak (obviously it critically depends on the scenario we are dealing with), but there is always a primary component: that of the surface reflection.

However, for most terrestrial applications, the "two-ray model" assumes a flat Earth, but this can be inaccurate for A2Gapplications, particularly when the link distances exceed a few tens of kilometres. This then requires the more complex "curved-Earth two-ray model" (CE2R), the geometry of which can be seen in *Fig.2.b* (an accurate analysis of the CE2R model appears in [12]).

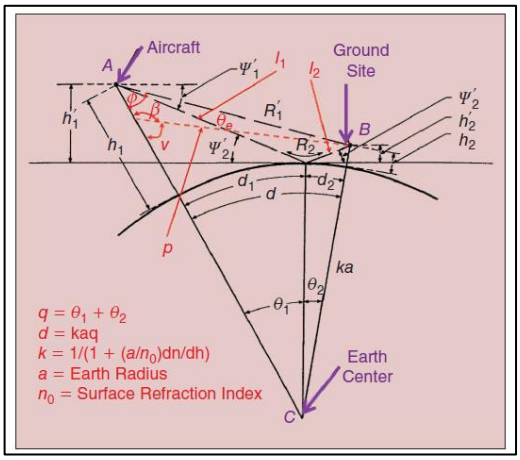

Figure 2.b Physics behind the CE2R

As a summary, the CE2R model accounts for many variables and it becomes more reliable even with bigger distances (obviously it is still inaccurate when additional MPCs are present). For instance, it considers the surface electrical characteristics, spherical wave divergence, and surface roughness. Additional considerations, such as ducting, foliage attenuation, atmospheric gas attenuation are discussed in [12], but they all are effects which occur with a small probability or at least have a minor impact on the A2GChannel in our bands.

So, due to its simplicity and reliability (we assume some limited cases) the full CE2R model path loss in decibels could be useful and it is given by:

$$\boldsymbol{L_p} = 20\log\left[\frac{4\pi d}{\lambda}\right] - 20\log\{|1 + rD\Gamma\exp\left[\frac{-j2\pi\Delta R}{\lambda}\right]|\}$$

Where *d* is the link distance, λ is the wavelength, *r* is the surface-roughness factor, *D* is the divergence factor due to the spherical Earth, Γ is the surface reflection coefficient and ΔR is the relative path length difference between the LOS and surface reflection.

2.2.4 Modeling Approach.

After collecting measurement data, a model can be developed for various settings. Then, parameters are extremely important, and they can depend on as many features as practical (e.g. Ground Station setting, elevation angle, etc.). Hence, a complete model can be in form of time-varying channel impulse response (CIR as said before), or its Fourier transform, the time-varying transfer function.

Another desirable attribute of a model is that it can be employable in computer simulations, and for this we could use the several model types analysed before (other models are described in [13]).

2.3 The Air-to-Ground Channel: Different Scenarios.

2.3.1 Why different scenarios?

As already said, the use of UAVs is growing rapidly. To ensure safety, UAV control and CNPC links must operate very reliably in a variety of conditions. This requires an accurate quantitative characterization of the A2Gchannel and, therefore, an analytical model which best fits the work environment.

Hence, the scenario assumes an extremely important role in characterizing the A2GChannel and the model we use clearly depends on it.

As with terrestrial cellular channels, classification of the various types of A2GChannels presents ambiguities and overlaps. Anyway, in most cases, scenario can be classified considering two aspects:

- Type of terrain: it can be flat, hilly, mountainous, over water.
- Type of environment: rural, sub-urban, urban.

Obviously, these classifications are not always disjoint and are not necessarily exhaustive, so a complete analysis of the specific environment is often needed.

In this chapter, two scenarios are taken in consideration due to their importance and their use for practical applications.

2.3.2 Rural or Over-Water Scenarios.

These are probably the easiest scenarios to deal with. That is because there are no obstacles nor particular constraints. Furthermore, the absence of random objects in LOS trajectory means no additional MPCs (there is just the principal one reflected by the terrain or the sea, see *Fig. 2.c*).

As illustrated in [14], in an open Over-Water setting propagation, PL follows the free-space increase with distance, but significant deviations (<10 dB) from this linear decibel increase with long distance arise from the strong water surface reflection. Hence, the CE2R model is more accurate than a free-space PL model.

To get better results, the model can be augmented with the Rician fading (adding a K-factors depending on the frequency band analysed).

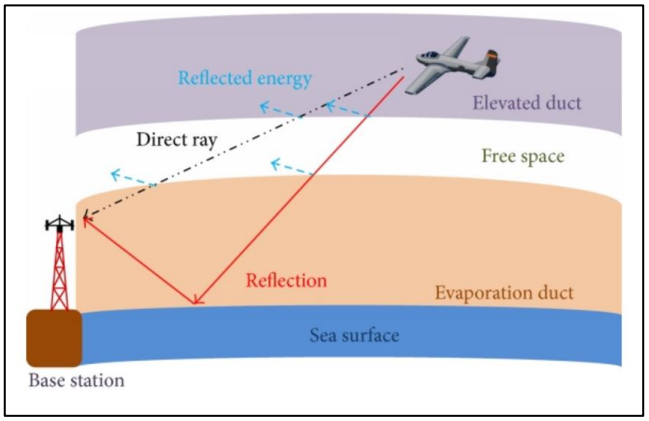

Figure 2.c Example of an Over-Water Scenario

2.3.3 Urban Scenarios.

These scenarios are, instead, the hardest to analyse and the reason is mainly due to the MPCs arisen from the reflections of signals on the obstacles. (*Fig. 2.e*). In fact, in complex environments like the urban one, infrastructural elements as buildings, bridges, railway stations, airports, etc. can heavily affect the propagation of electromagnetic signal with respect to the free space case. In these environments, the field propagation is dominated by multipath (the MPCs) (look for further information [15]) and many replies of the same signal arrive at the receiver from different directions and with different time delays.

Moreover, these types of scenarios are fundamental because of their practical applications. In fact, one of the most attractive use of drones' technology is in telecommunication and therefore their employment in crowded and full of obstacles environments.

Hence, even though the study of an A2GChannel in urban scenarios could be a very hard challenge, a complete analysis is strongly needed.

And for this purpose, two steps are taken into account:

- Modeling Urban Environment using the existing ITU-R Model for urban areas;

- The optimal Low Altitude Platform (LAP) for Maximum Coverage.

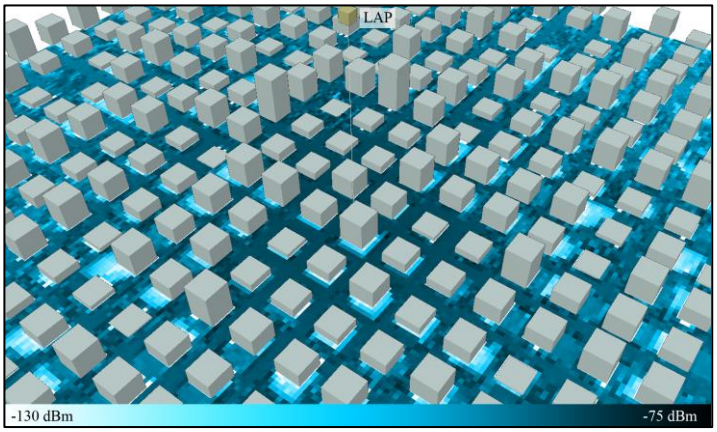

Figure 2.d Example of an Urban Scenario. A LAP is hovering the city and the lighter is the blue the less is the Received Power

2.3.3.1 Modeling Urban Environment.

Few literature papers are available on characterizing the Air-to-Ground propagation over urban environment. The most comprehensive work in this regard can be found in [16] and [17], where the authors proposed that A2Gcommunication occurs in accordance to two main propagation groups.

In fact, due to the buildings, signals are often split into other types of rays (direct, diffracted and reflected), but to simplify the calculations, in this elaborate only two propagation groups will be analysed (for a statistically derivation [16]):

- The first group corresponds to receivers favouring a LoS condition.
- The second one corresponds to receivers with no LAP LoS but still receiving coverage via strong reflections and diffractions (NLoS condition).

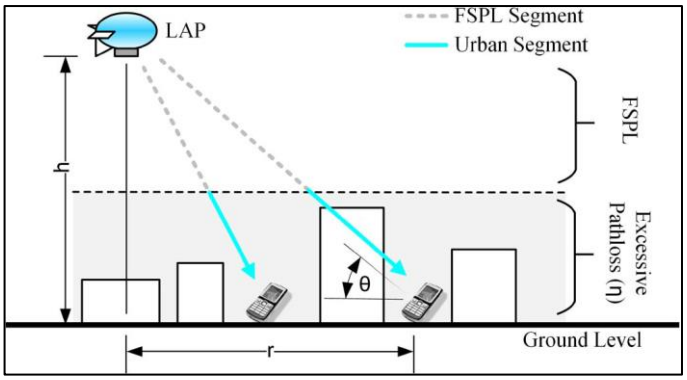

Figure 2.f Example to highlight the difference between the Free Space Path Loss Segment and the Urban Segment

As shown in *Fig.f* radio signals emitted by a LAP base station propagate in free space (FSPL represents the Free Space Path Loss) until reaching the urban environment where they incur shadowing and scattering caused by the man-made structures, introducing additional loss (the Excessive Pathloss η refers to the mean value of the PL depending on the propagation group). Finally, the angle θ is the "elevation angle" between the user and the LAP base station.

Hence, the main step for modelling the Urban Environment is firstly analyse the LoS probability. The International Telecommunication Union (ITU) in [18] suggests a remarkable method for finding the probability of geometrical LoS between a terrestrial transmitter at elevation h_{TX} and a receiver at elevation h_{RX} in an urban environment.

The results (a complete analysis is in [19]) can be closely approximated to a Sigmoid function (S-curve) of the following form:

$$\boldsymbol{P(LoS, \theta)} = \frac{1}{1 + a\ exp\ (-b[\theta - a])}$$

Where a and b are called here the S-curve parameters. With this formula calculation become much easier and an accurate approximation of a real situation is showed in *Fig.2.g*, where the probability is plotted for different urban environment.

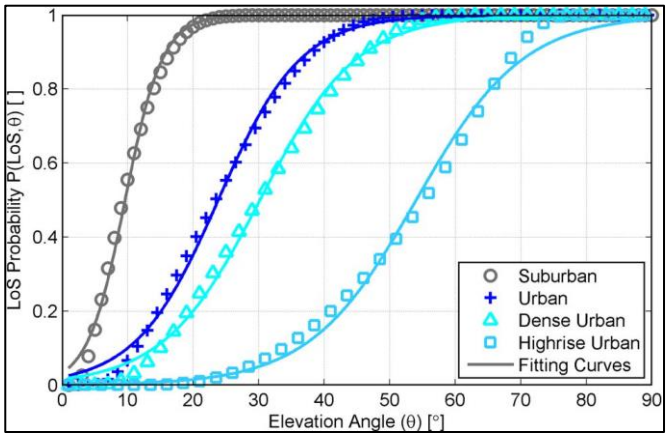

Figure 2.g Plot for the LoS Probability as a function of the Elevation angle. The denser is the scenario, the lower is the Los Probability.

Once calculated the LoS probability, for modelling an urban environment, we need a Radio Model Implementation (a detailed discussion in [20]). It is fundamental to choose the right parameters, whether we are in a normal urban area, a Dense Urban area or a Highrise Urban area. Also, parameters depend the work frequency too.

2.3.3.2 Optimal LAP for Maximum Coverage.

Low Altitude Platforms (LAP) [21] are quasi-stationary aerial platforms (Quadcopters, UAVs or balloons) with an altitude below the stratosphere (10,000 m), in contrary to High Altitude Platforms (HAP) [22] that can reach the upper layers of the stratosphere.

The reason LAPs are more suitable in this elaborate is that in general, they are much easier to deploy, and are inline with the broadband cellular concept, since low altitude combines both coverage superiority and confined cell radius.

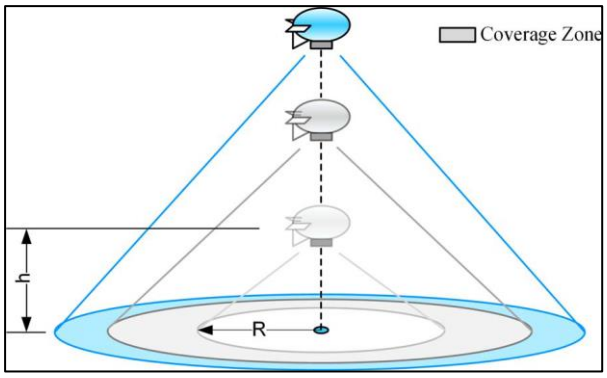

Figure 2.h Coverage Zone as a function of the height

Hence, it is clear that an A2G Channel for a UAV in an urban environment follows the rules of the LAPs with the right parameters (depending on work frequency and the type of urban scenario). So, an augmented efficiency of the drones' possibilities would be useful. That is why in a remarkable paper [19] the optimal altitude is calculated for a LAP to maximize the coverage. The author starts from the concept of maximum allowable pathloss (the PL_{max}) because as

depicted in *Fig. 2.h* when the total pathloss between the LAP and a receiver exceeds this threshold, the link is deemed as failed. And for ground receivers this threshold translates into a coverage disk of radius *R*, inside which all receivers have a PL less than or equal to PL_{max}.

To calculate it, the author begins with the simple Friis Formula (isotropic receiver and transmitter) and adds the excessive pathloss for each propagation group (as already said these groups are simply the LoS and NLoS):

$$\boldsymbol{PL_{LoS}} = 20\log d + 20\log f + 20\log\left(\frac{4\pi}{c}\right) + \eta_{LoS}$$

$$\boldsymbol{PL_{NLoS}} = 20\log d + 20\log f + 20\log\left(\frac{4\pi}{c}\right) + \eta_{NLoS}$$

Where *d* is the distance between the LAP and a receiver at a circle of radius *r*, while *f* is the system frequency. Then, knowing the LoS probability and assuming the NLoS probability as following:

$$P(NLoS, \theta) = 1 - P(LoS, \theta)$$

He indicates the PL_{max} in this simple way:

$$PL_{MAX} = P(LoS) * PL_{LoS} + P(NLoS) * PL_{NLoS}$$

Or rewriting with the previous equations, this is the final formula:

$$\boldsymbol{PL_{MAX}} = \frac{A}{1 + a\exp(-b[\theta - a])} + 20\log(Rsec\theta) + B$$

Where $\boldsymbol{A} = \eta_{LoS} - \eta_{NLoS}$ and $\boldsymbol{B} = 20logf + 20log(4\pi/c) + \eta_{NLoS}$.

Finally, to calculate the optimum altitude (h_{OPT}) that yields the best coverage, we just need to satisfy this equation:

$$\frac{dR}{dh} = 0$$

In *Fig. 2.i* it is plotted the variation of *R* with respect to *h* for the four urban environments, highlighting the h_{OPT} for each of them.

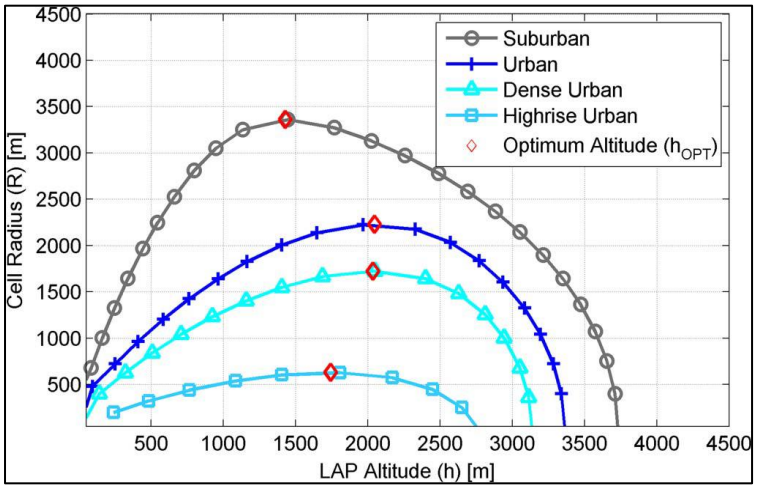

Figure 2.i Plot of the Cell Radius as a function of the LAP altitude to highlight the Optimum Altitude.

2.3.4 Factory Scenarios.

This type of scenario has a fundamental role for this thesis because it represents one of the environments where the measurement campaign took place.

Physically speaking, a factory scenario is a very complex environment where a lot of obstacles occur very frequently. This means that the propagation of signal is very affected and many MPC arise from reflections and diffractions. Furthermore, differently from the urban scenarios, there are a lot of metal objects which can more efficiently reflect the electromagnetic signals (the reflection coefficient is usually similar to one).

Talking about future applications, studying the propagation of mmWave in these scenarios could be helpful for all the so-called "4.0 industries", to control for instance machines and robots and to connect all of them in a single network.

CHAPTER 3

THE ULTRA-WIDE BAND RADIO TRANSCEIVER

3.1 Ultra-Wide Band Overview.

3.1.1 The Ultra-Wide Band Technology and Advantages.

The Ultra-Wide Band (UWB) is a radio technology which can use a very low energy level for a short-range, high bandwidth communication over a large portion of the radio spectrum. This is possible because very short-perioded pulses are used and therefore, the signal will have a very large frequency bandwidth. Moreover, thanks to the extremely low average power, these devices are usually very energy-efficient, but can be used just for low distances.

The very short-perioded pulses of an UWB technology give to these devices numerous advantages:

- *Sharing of frequency spectrum*. The constraints of transmission Power Spectral Density are on -41.3 dBm/MHz (75 nW/MHz). Hence, the UWB systems are usually below the noise threshold and this means that more devices can work at same frequencies without interfering.
- *High Data-Rate.* The large frequency bandwidth leads to a high Channel Capacity, which is the quantity of data transmitted per second on a channel. This can be clearer in this formula (Hartley-Shannon formula for added White Gaussian noise):

$$\boldsymbol{C} = B \log_2(1 + \frac{S}{N_0 B})$$

Where *C* is the maximum capacity of channel, *B* is the band, *S* is the signal Power and N_0 is the power spectral density of noise.

- *Low probability of interception.* This is thanks to the very low average power.
- *High efficiency against Multi-Path.* The information can be received in a very short time, so the LoS signal is likely to be not disturbed by the others, which can be isolated.
- *Simple architecture for the transceiver.* Since UWB systems are based on the transmission of short pulses, it means that the modulation of the sine carrier is not necessary. The hardware parts are simplified too, because no mixer or local oscillator are needed. Hence, information is transmitted just with pulses' modulation, usually with some technics such as PPM (Pulse Position Modulation) and PAM (Pulse Amplitude Modulation). [23]

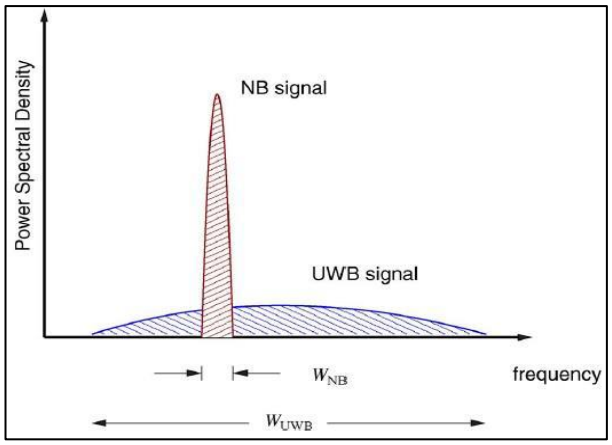

Figure 3.a Plot to highlight the wide band of an UWB signal. With a low Power Spectral Density we have a very huge band

3.2 The Time Domain - PulsON® 410.

3.2.1. Basic Functions and How to control.

The P410 is an Ultra-Wideband (UWB) radio transceiver and/or radar sensor that provides the following functions:

- It accurately and reliably measures the distance between two P410s and provides these measurements at a high update rate (communication data between two or more P410s is also permitted);

- It supports two different range measurement techniques (Two-Way Time-of-Flight and Coarse Range Estimation);
- RF transmissions from 3.1 GHz to 5.3 GHz, with center at 4.3 GHz
- It is also possible to operate the P410 as hybrid device that is both a ranging radio and a radar sensor.

The user can control the P410 through an Application Programming Interface (API) over USB or Serial connections. Moreover, demonstrating the performance is also possible through two PC-based Graphical User Interfaces (GUIs) which provide programmers with a visual example of a host application which interfaces to the P410 through the API.

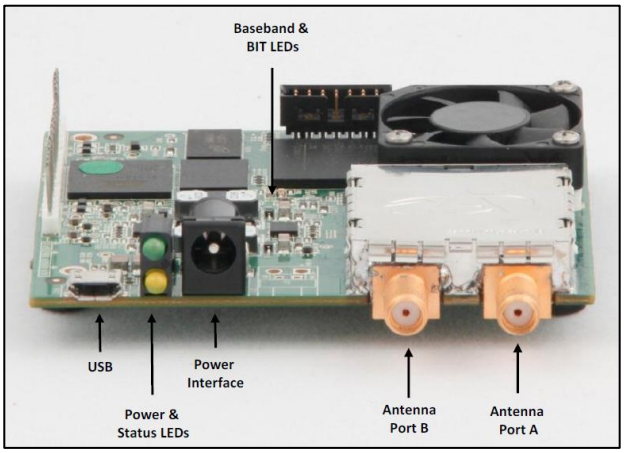

Figure 3.b Side view of the P410 RCM displaying connections

3.2.2. Typical Use of the P410 radio transceiver.

This device is extremely precise and can be used in various applications.

- *As a ranging radio*, more useful for our measurement campaign. It is a low power and affordable device which provides accurate, high rate range measurements and superior operational performance when compared to conventional RFID/RTLS devices. (*Fig. 3.c)*

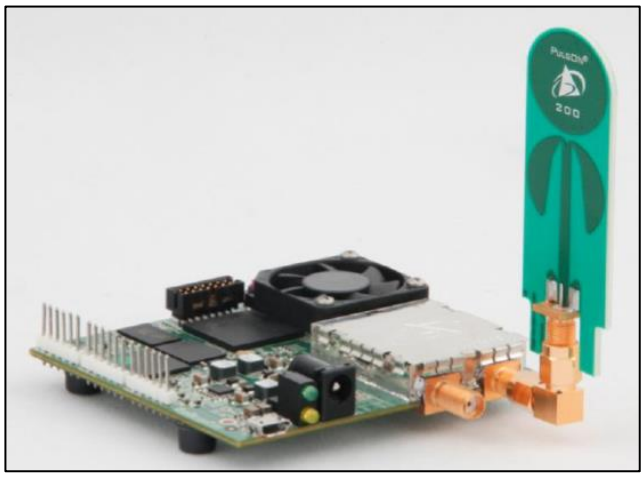

Figure 3.c P410 used as a Ranging Radio

- *As a monostatic radar*, less useful for our purpose. It is a low-power and affordable monostatic radar platform that provides more than one GHz of radio frequency bandwidth at a center frequency of approximately 4 GHz. (*Fig. 3.d*)

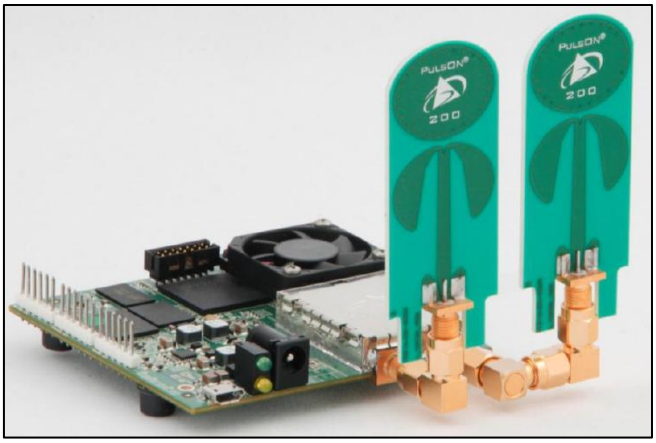

Figure 3.d P410 used as a Monostatic Radar

CHAPTER 4

THE MILLIMETER WAVE RADIO TRANSCEIVER

4.1 Millimeter Wave Overview.

4.1.1. The Millimeter Wave Technology and Advantages.

Microwave cellular systems have precious little spectrum. (see [24] for further details).

Obviously there are some ways to gain more spectrum such as refarm spectrum or using cognitive radio techniques [25] alternatively there is an enormous amount of spectrum at mmWave frequencies ranging from 3 to 300 GHz.

The enormous amount of spectrum is just one of the advantages of this type of technology. For the 5G for instance, mmWave could be implemented with other features which can improve exponentially the quality of the nowadays communication.

- Antenna arrays are key feature in mmWave systems. Large arrays can be used to keep the antenna aperture constant, eliminating the frequency dependence of PL to omnidirectional antennas.
- Adaptive arrays with narrow beam also reduce the impact of interference: mmWave systems could operate in noise-limited rather than interference-limited conditions.
- MmWave operation is seen to provide very high rates compared to two different microwave systems. The gains exceed the 10x spectrum increase because of the enhanced signal power and reduced interference thanks to directional beamforming at both Tx and Rx.

4.2 The SAF Tehnika mmWave Measurement Kit.

4.2.1 Basic Functions and typical use.

Basically, as you can see in *Fig.4.a,* the SAF Tehnika Measurement Kit consists on a receiver (the Spectrum Compact Analyser), and a transmitter (the Signal Generator Compact), then there are different types of antennas, SMA connectors and RF cables.

To analyse data, instead, we need a PC software called "Spectrum Manager".

The Spectrum Compact is an ultra-light and easy to use measurement solution. It operates in a frequency range of 2-40 GHz. It is a battery-powered device, suitable for any outdoor use e to perform actual installation of the link or gathering data for site planning purposes. It has an LCD touchscreen which ensures intuitive use of spectrum analyser and can be connected directly to any antenna via SMA connector.

Figure 4.a The SAF Tehnika Spectrum Analyser (receiver) and The Signal Generator (transmitter)

4.2.2 The Spectrum manager.

Spectrum Manager (*Figg. 4.b and 4.c*) is a free PC software designed for use with SAF Tehnika Spectrum Compact, E-band Spectrum Compact and V-band Spectrum Compact spectrum analysers. Spectrum Manager allows to work with

saved Spectrum Compact Curves (files have an extension ".scc") and Spectrum Compact Curve Recordings (extension ".rsc").

Hence, to convert into files with ".csv" (Comma Separated Values) extension, which can be more easily analysed, a Matlab script is needed (see chapter 5.2.4).

Figure 4.b Analyzing the spectrum with the horn antenna

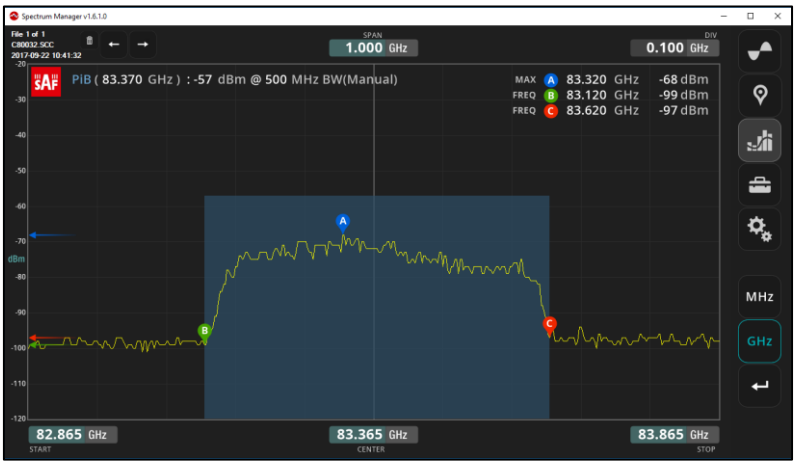

Figure 4.c Example of a Spectrum analyzed with Spectrum Manager

CHAPTER 5

MEASUREMENT CAMPAIGN IN FACTORY ENVIRONMENT

5.1 Introduction.

5.1.1. Introduction for the Measurement Campaign.

The aim of this Measurement Campaign is simply to put into practice what we already know about physics behind the behavior of signals and their propagation in interesting scenarios at different frequencies. In this specific case, we studied the propagation in a factory, a rich of scattering environment where obviously signals are subjected to a large amount of reflections and diffractions.

For instance, we studied the signal distribution of power, the "Power Angle Profile" and we found that it is quite easy even with high frequencies (a principal lobe in LoS condition and size lobes due to the principal reflections). Similarly, we know we can obtain the time distribution, the "Power Delay Profile", from the impulse response which has few principal peaks.

Hence, we analyzed the behavior of signals with two different frequency-bands: the Ultra-Wide Band (center frequency at 4.3 GHz) and the Millimeter Wave Band (27 or 38 GHz) in order to implement, in the future, smarter and smarter technologies such as dynamic antennas, directive antenna arrays and directional beamforming .

So, we could split this measurement campaign into two different experiments with two different measurement setups:

- The Millimeter Wave Measurement Setup. Where we used a rotating receiver (with a horn directive antenna) and a fixed transmitter (with an

omnidirectional antenna) in twenty-four different combinations. See for details chapter 5.2.1.

- The Ultra-Wide Band Measurement Setup with the drone. Where we put a transmitter on the drone (with an omnidirectional antenna) and another omnidirectional antenna was stationary (in different positions). The drone was hovering or doing a scheduled trajectory. See for details chapter 5.3.1.

5.1.2. The Factory in Pontecchio Marconi (BO).

Thanks to a Professor's friend we could stay for our experiments in a factory specialized in automation machines in Via Primo Maggio, 11/5, Pontecchio Marconi, Bologna. (a google map image in *Fig. 5.a*)

Figure 5.a. Top view of GF Automazioni factory in Pontecchio Marconi

The place is quite interesting for our purpose due to a huge amount of metallic shelves, tables, cupboards and stuff of different sizes. (see *Figg. 5.b and 5.c*) This means that we could consider some of these obstacles as scatterers and study how much propagation of signal is affected. Moreover, the presence of potential reflections and diffractions creates different MPCs which make this environment very similar to the general description of a factory scenario.

Figure 5.b Right Side of the factory

Figure 5.c. Left Side of the factory

5.2 The Millimeter Wave Setup Measurement.

5.2.1. Description of the experiment.

The concept of this experiment is quite easy: with the SAF Tehnika measurement kit, we analysed the received Power Angle Profile (PAP) for different situations and positions.

Studying the PAPs, especially in these complex scenarios, is very useful to better understand the potential performance of beamforming techniques, where smart antennas can adapt their beam pattern dynamically.

Hence, in this experiment, for each Rx position (three in total), we took measurement with eight different Tx position, and for each *Rx_Tx* combinations we rotated the receiver with 15 degrees steps. In *Fig. 5.d*, a map of the factory on scale shows all the different positions of the antennas with all distances and dimensions.

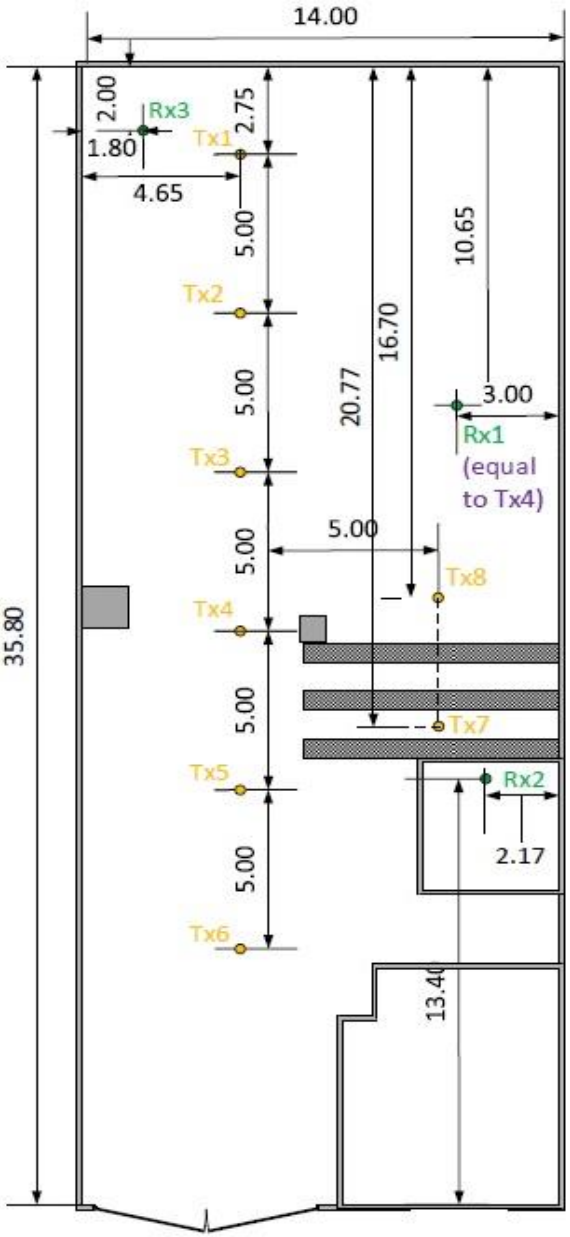

Figure 5.d Map of the factory

Figure 5.e The YAESU motor on the tripod of the receiver

5.2.2. Equipment for the experiment.

The equipment we used for this experiment is explained below:

- The *SAF Tehnika Spectrum Compact Analyser*, which is basically the receiver. It shows an instantaneous plot in which the horizontal axis represents a linear frequency scale and the vertical axis is a logarithmic power scale. Obviously there is also a menu with some intuitive buttons to set up spans, markers or customize plots.

  For this experiment we used the version *"JOSSAP14"* with a *frequency range* from 24 to 40 GHz, an *Input Power range* from -100 dBm to -40 dBm and a fixed *Resolution bandwidth* of 1 MHz.
- A Rotor for the antenna receiver mounted on the tripod. (*Fig. 5.e*). We used a *"YAESU G450C"* with both manual control and digital control thanks to a PCB (the *ERC RS232 V4.0*) soldered and placed inside the motor. See for details chapter 5.2.3.
- The Conical Horn antenna for SAF Spectrum Compact. We used the version *"J0AA2640HG03"*, with an *operating frequency* from 26.5 to 40.5 GHz and a typical *Gain* of 21 dBi. (*Fig 5.f*)
- The *SAF Tehnika Signal Generator Compact*, which is the transmitter. With the touchscreen display the frequency of the signal can be easily chosen and in the same way the Output power too.

  The version we used is *"JOSSAG14"* with a *frequency range* from 24 to 40 GHz, an *Output Power range* from -3 dBm to 5 dBm and a Continuous wave as the *Signal form.*
- Two tripods for the receiver and transmitter.
- SMA connectors and RF cable.

Figure 5.f The Conical horn antenna used as a receiver

5.2.3. A Rotor for the antenna receiver: the YAESU G450C.

In order to calculate the Power Angle Profile (PAP), we need the received power for different angulation. Hence, the idea was to use a motor mounted on the tripod of the receiver, so that we could make shots and save the received power every 15 degrees step (in total: 360°/15° = 24 shots).

The YAESU rotor was quite nice: a display shows the azimuthal polarization and two buttons can be used to rotate the antenna clockwise or vice versa. (*Fig. 5.g*)

However, pressing buttons mechanically would have been a bad solution and a waste of time.

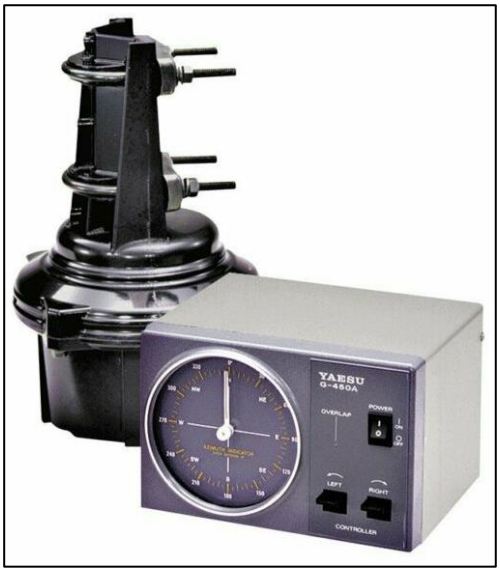

Figure 5.g The YEASU G450 Rotor

Hence, we built a PCB which basically emulates the physical buttons, so that we could start every rotation form a PC command (with a Rotor Control software).

The PCB is called *ERC RS232* and thanks to it, the rotor became partially digital and we could save a lot of time.

I soldered personally the PCB, (*Fig. 5.h*) controlled the number of pieces through the Data Sheet *(Fig. 5.i*) and as soon it was completed (*Fig. 5.j*), finally mounted inside the rotor. (*Fig. 5.k*).

Afterwards, the rotor is simply mounted on the tripod and thanks to the PC software (the Electronic Rotor Control) we could rotate the antenna receiver via digital inputs. (*Fig. 5.l*)

Figure 5.h The Soldering station with the tin and flux.

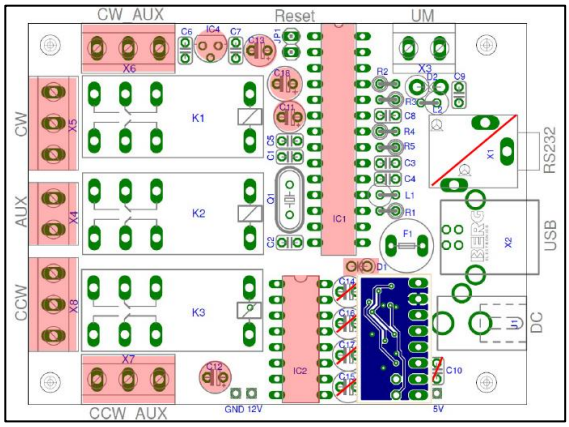

Figure 5.i Scheme of Components.

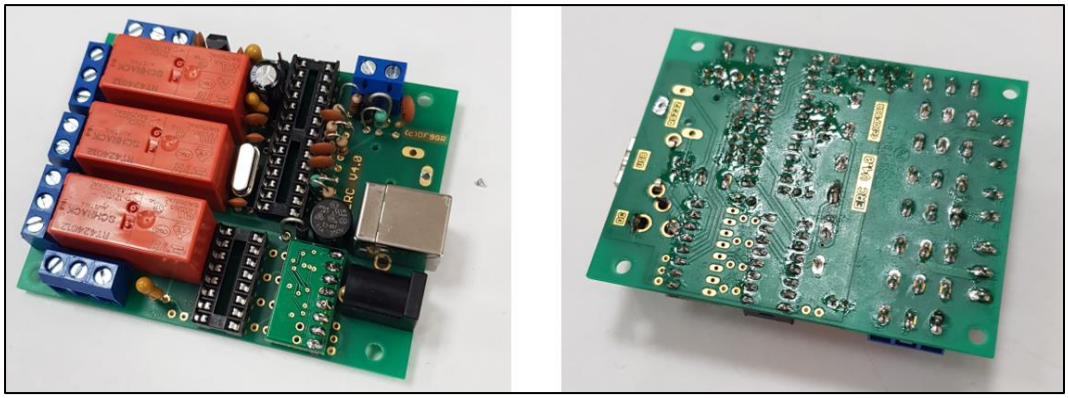

Figure 5.j The PCB completed.

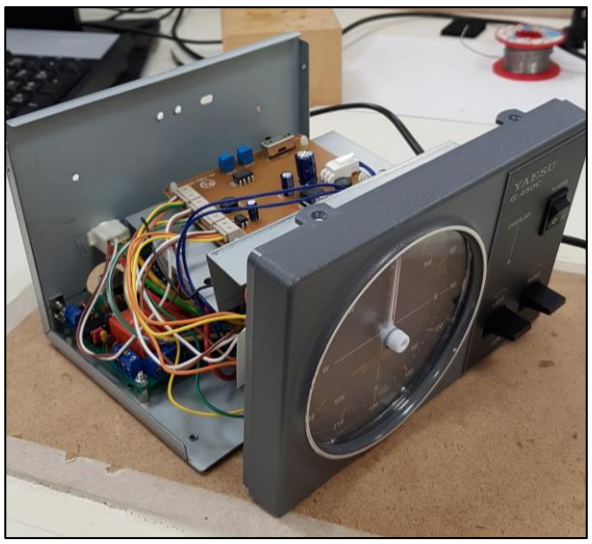

Figure 5.k The PCB inside the rotor.

Figure 5.l The ERC software interface

5.2.4. The Power Angle Profile (PAP).

This is perhaps the most interesting part of the experiment. The Power Angle Profile (PAP) is basically a function on an angular domain, which expresses power (usually in dBm) as a function of the angle.

This value is quite fundamental to have a good prospective for future challenges in building adaptive antennas and beamforming.

The procedure to obtain the Polar PAPs, however, is quite mechanical, but basically easy:

- Collect all data into separate directories. In our case the situation was quite standard: first, the three receivers (*Rx1*, *Rx2* and *Rx3*), inside of each there were the eight transmitters (*Tx1*, *Tx2*.. *Tx8*), and finally inside of each transmitter twenty-four different Spectrum Compact Curve of Power (for 360°/15 steps = 24 files .scc).
- Convert all the Spectrum Compact Curves (.scc) into a Comma Separated Values (.csv) extension, in order to post-process them using Matlab. To do so, there is the option “save as-file extension .csv” in the Spectrum Manager software, unfortunately we did not find a faster way.
- Import data on Matlab and save them into a multidimensional matrix (“DATA”). Here is an example of Matlab script, suitable for our situation:

```
DATA = zeros(2,200,24,8,3);
for i = 1:3
    for j = 1:8
        folderName = ['RX',num2str(i),'\','TX',num2str(j)];
        openFolder = dir(folderName);
        nFiles = size(openFolder,1)
        for k = 3:nFiles
            %% File Name
            fileName = [folderName,'\',openFolder(k).name];
            dataTemp = csvread(fileName,2,3);
            DATA(1,:,k-2,j,i) = dataTemp(:,1:end);
        end
    end
end
```

- Isolate only the maximum value ("idxmaxFreq") of each .csv files and put them into three different Matrices. In the end, there will be 3 Matrices 8x24 ("data").

  Here is an example of Matlab script for our situation:

```
L = size(DATA,5); % n. of RXs
M = size(DATA,4); % n. of TXs
N = size(DATA,3); % n. of measured angulations

[maxval,idxmaxFreq] = (max(DATA(1,:,1,1,1)));

powCentralFreq = zeros(N+1,M,L);
for l = 1:L
    for m = 1:M
        for n = 1:N
            powCentralFreq(n,m,l) = DATA(1,idxmaxFreq,n,m,l);
        end
        powCentralFreq(N+1,m,l) = powCentralFreq(1,m,l);
    end
end

data = powCentralFreq(:,:,:);
```

- For the *Average Azimuth Arrival Angle* ("meanPhi") and the *Angular Spread* ("rmsPhi"), here is an easy Matlab script:

```
Pi = 10.^(data(1:N,:,:)./10);
Pt = squeeze(sum(Pi,1));

meanPhi = zeros(N,M,L);

for l = 1:3
    for m = 1:8
        for n = 1:24
            meanPhi(n,m,l) = phiRad(n)*Pi(n,m,l)/Pt(m,l);
        end
    end
end

meanPhi = squeeze(sum(meanPhi,1)); %Avg azimuth arrival angle in rad
meanPhiDeg = (meanPhi.*180)./pi    %Avg azimuth arrival angle in deg

rmsPhi=zeros(M,L);
for w = 1:3
    for m = 1:8
      rmsPhi(m,w) = std(phiRad(1:N),squeeze(Pi(:,m,w)./Pt(m,w)));
    end
end

rmsPhiDeg = (rmsPhi.*180)./pi;     %Angular Spread in deg
```

- In the end, to easily analyse the Power Angle Profile (PAP), we plotted some Polar PAPs, which are quite useful. The script we used is shown below:

```
phiRad = (0:360/N:360)*pi/180;

figure;

for l = 1:L                                  % n. of RXs
    for m = 1:M                              % n. of TXs

      currData=squeeze(data(:,m,l))-min(squeeze(data(:,m,l)));
      a=linspace(min(currData)-2,max(currData)+2,7);
      a=a+min(squeeze(data(:,m,l)));

      polarplot(phiRad,currData,'r','Marker','o',...
      'MarkerSize',5,...
      'MarkerFaceColor','k');

      ax=polaraxes;                          %Axis Properties
      ax.ThetaZeroLocation='top';            %Zero degree on top
      ax.ThetaDir ='clockwise';              %Clockwise rotation

       rlim([min(currData)-2 max(currData)+2]);
       a=a-min(squeeze(data(:,m,l)));
       rticks(a);
       a=a+min(squeeze(data(:,m,l)));
       rticklabels({num2str(round(a(1))),num2str(round(a(2))),...
       num2str(round(a(3))),num2str(round(a(4))),num2str(round(a(5))),...
       num2str(round(a(6))),num2str(round(a(7)))})

    end
 end
```

5.2.5. Results and Conclusions.

An interesting result for this experiment is inside every Polar Plot: the distribution of power is quite easy. There is a main lobe in the LoS direction, and the size lobes are quite always associated to a strong reflection by the closest wall.

In the maps, I simply overlaid the PAPs we got from 27 GHz with the PAPs from 38 GHz. The result is twenty-four Polar PAPs: eight maps with three plots each.

The *Input Power* was 5 dBm, *Sweep Time* was 0.9 sec and as already said, the transmitter was a fixed omnidirectional antenna and the receiver was a rotating directive antenna (with shots every 15 degrees step).

In the maps, the centers of the polar PAPs are placed right above every Rx.

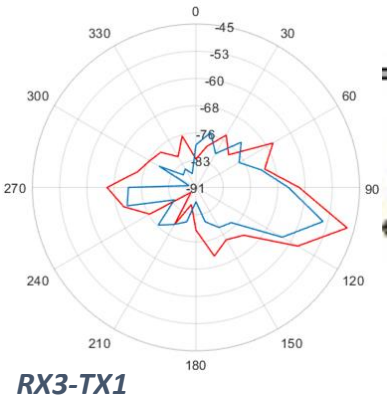

TX1

LEGEND RXi_TX1

38 GHz

27 GHz

RX3-TX1

Avg. Azimuth arrival angle:

108.87 deg 110.01 deg

Azimuth Spread (Std Deviation):

26.51 deg 33.59 deg

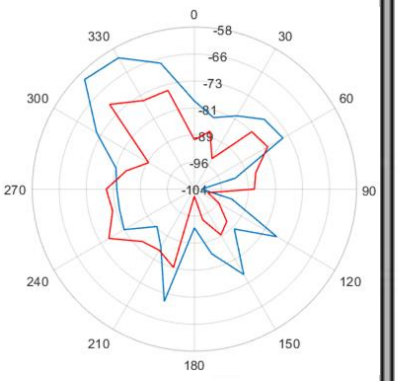

RX1-TX1

Avg. Azimuth arrival angle:

294.19 deg 303.36 deg

Azimuth Spread (Std Deviation):

70.50 deg 63.76 deg

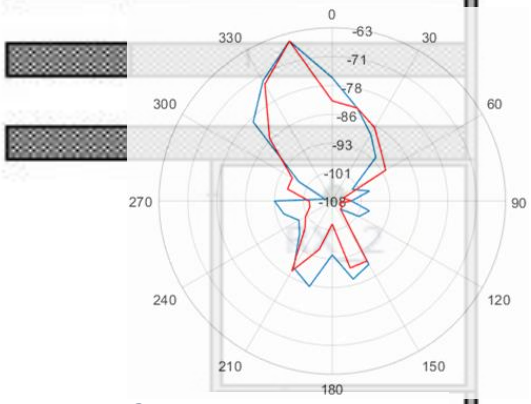

RX2-TX1

Avg. Azimuth arrival angle:

327.69 deg 312.89 deg

Azimuth Spread (Std Deviation):

66.29 deg 90.97 deg

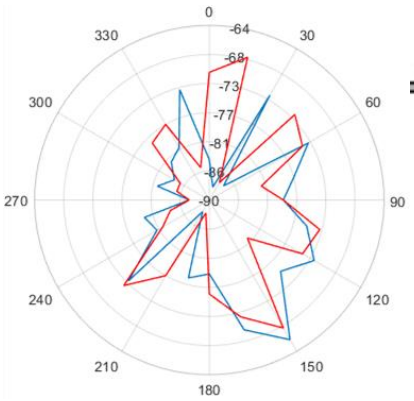

RX3-TX2

Avg. Azimuth arrival angle:

112.35 deg 153.72 deg

Azimuth Spread (Std Deviation):

88.67 deg 77.39 deg

LEGEND RXi_TX2

38 GHz

27 GHz

Tx2

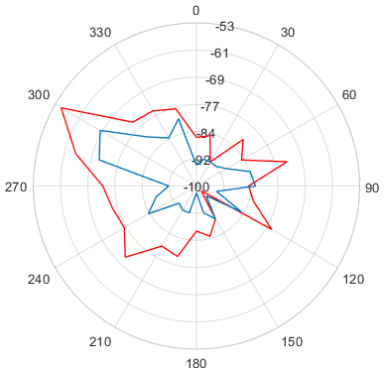

RX1-TX2

Avg. Azimuth arrival angle:

289.87 deg 283.46 deg

Azimuth Spread (Std Deviation):

38.41 deg 53.32 deg

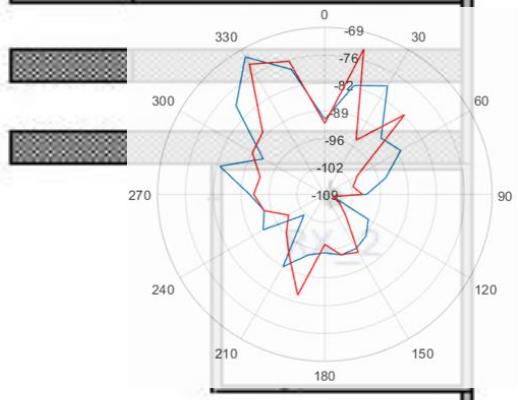

RX2-TX2

Avg. Azimuth arrival angle:

200.30 deg 275.54 deg

Azimuth Spread (Std Deviation):

152.25 deg 111.58 deg

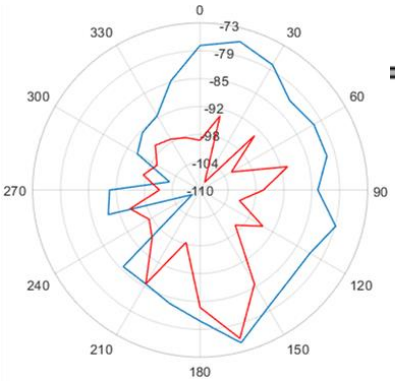

LEGEND RXi_TX3

38 GHz

27 GHz

RX3-TX3

Avg. Azimuth arrival angle:

166.47 deg 102.21 deg

Azimuth Spread (Std Deviation):

41.60 deg 80.12 deg

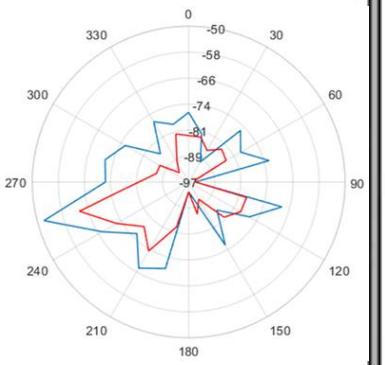

RX1-TX3

Avg. Azimuth arrival angle:

237.14 deg 245.48 deg

Azimuth Spread (Std Deviation):

49.65 deg 38.46 deg

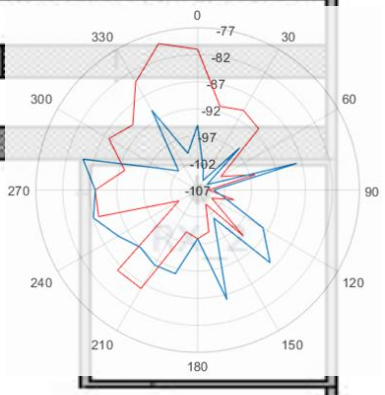

RX2-TX3

Avg. Azimuth arrival angle:

220.94 deg 207.89 deg

Azimuth Spread (Std Deviation):

138.65 deg 80.52 deg

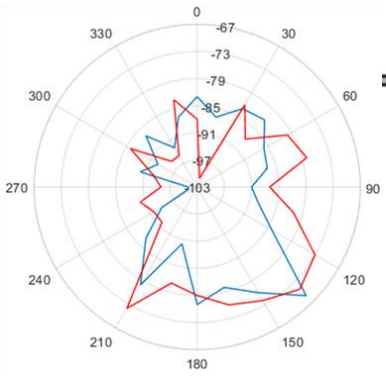

LEGEND RXi_TX4

38 GHz

27 GHz

RX3-TX4

Avg. Azimuth arrival angle:

150.72 deg 142.32 deg

Azimuth Spread (Std Deviation):

53.59 deg 51.23 deg

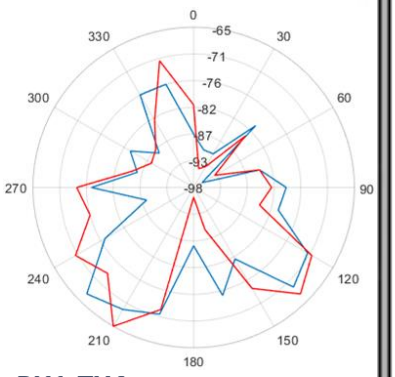

RX1-TX4

Avg. Azimuth arrival angle:

198.19 deg 193.29 deg

Azimuth Spread (Std Deviation):

65.76 deg 62.21 deg

RX2-TX4

Avg. Azimuth arrival angle:

249.55 deg 211.15 deg

Azimuth Spread (Std Deviation):

107.10 deg 60.95 deg

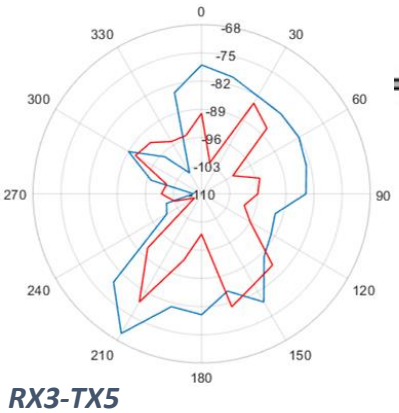

LEGEND RXi_TX5

38 GHz

27 GHz

RX3-TX5

Avg. Azimuth arrival angle:

159.59 deg 160.89 deg

Azimuth Spread (Std Deviation):

74.25 deg 82.35 deg

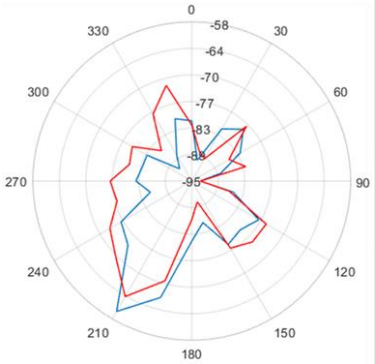

RX1-TX5

Avg. Azimuth arrival angle:

214.40 deg 202.71 deg

Azimuth Spread (Std Deviation):

61.86 deg 36.90 deg

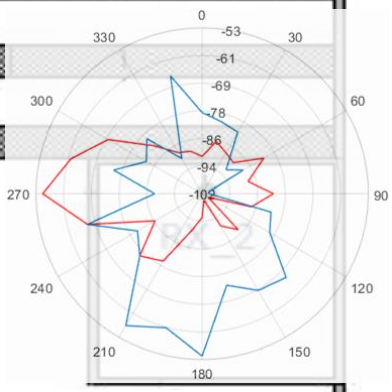

RX2-TX5

Avg. Azimuth arrival angle:

270.53 deg 194.89 deg

Azimuth Spread (Std Deviation):

19.31 deg 37.04 deg

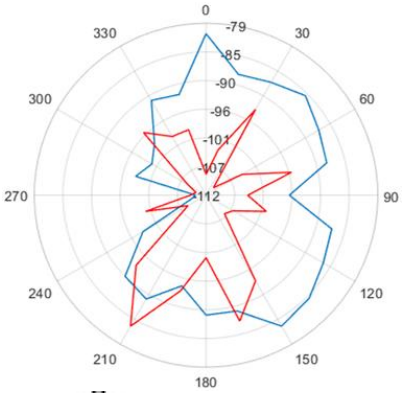

LEGEND RXi_TX6

38 GHz

27 GHz

RX3-TX6

Avg. Azimuth arrival angle:

188.72 deg 100.40 deg

Azimuth Spread (Std Deviation):

59.69 deg 84.65 deg

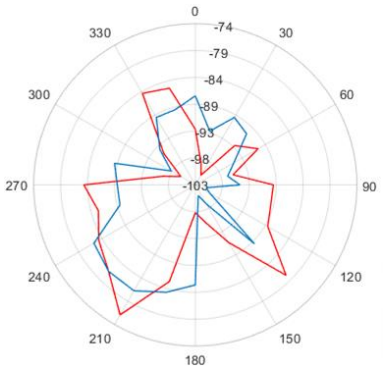

RX1-TX6

Avg. Azimuth arrival angle:

209.68 deg 201.09 deg

Azimuth Spread (Std Deviation):

66.02 deg 77.68 deg

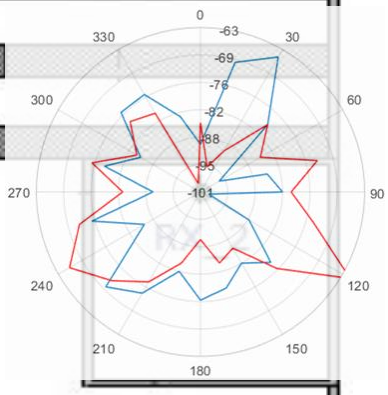

RX2-TX6

Avg. Azimuth arrival angle:

159.00 deg 118.27 deg

Azimuth Spread (Std Deviation):

64.71 deg 110.11 deg

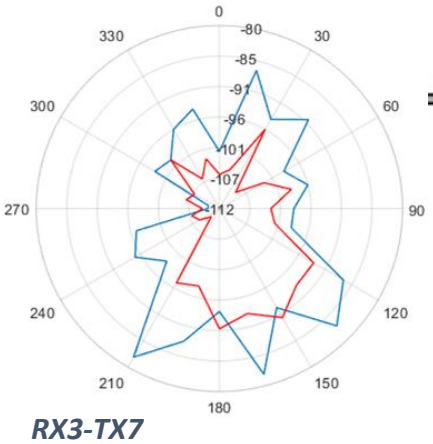

RX3-TX7

Avg. Azimuth arrival angle:

152.46 deg 155.96 deg

Azimuth Spread (Std Deviation):

58.74 deg 66.15 deg

LEGEND RXi_TX7

38 GHz

27 GHz

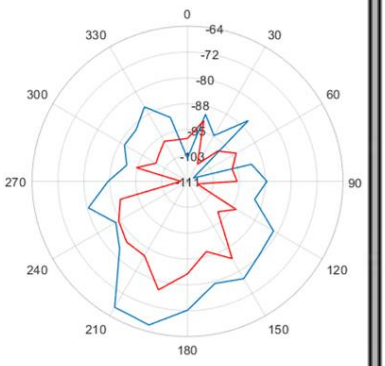

RX1-TX7

Avg. Azimuth arrival angle:

190.03 deg 195.67 deg

Azimuth Spread (Std Deviation):

43.20 deg 29.34 deg

RX2-TX7 (not centered)

Avg. Azimuth arrival angle:

252.19 deg 221.47 deg

Azimuth Spread (Std Deviation):

95.67 deg 26.99 deg

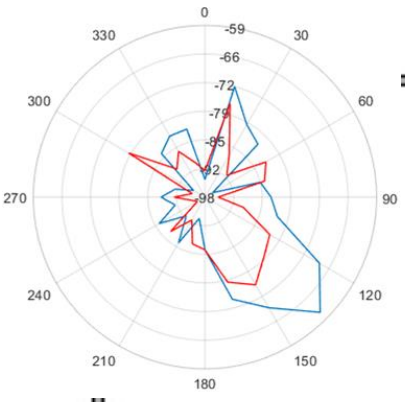

RX3-TX8

Avg. Azimuth arrival angle:

141.57 deg 130.81 deg

Azimuth Spread (Std Deviation):

91.07 deg 39.98 deg

LEGEND RXi_TX8

38 GHz

27 GHz

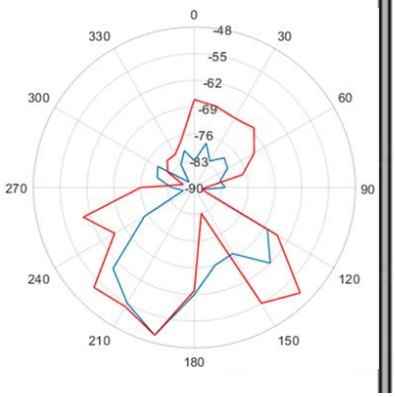

RX1-TX8

Avg. Azimuth arrival angle:

180.32 deg 195.43 deg

Azimuth Spread (Std Deviation):

43.18 deg 21.50 deg

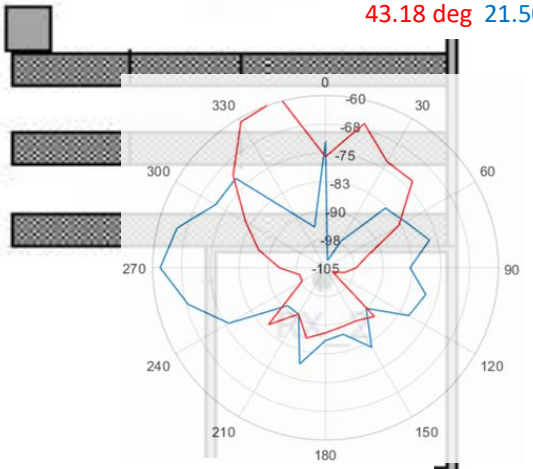

RX2-TX8

Avg. Azimuth arrival angle:

289.48 deg 252.38 deg

Azimuth Spread (Std Deviation):

114.15 deg 70.01 deg

5.3 The Ultra-Wide Band Setup Measurement.

5.3.1. Description & Equipment for the experiment.

The main purpose of this experience is studying not only the angular distribution of power (as we did in the previous experiment), but also the time distribution of signals in a rich of scattering environment. To do this, we used the best indoor localization system: the UWB signals.

As already said in chapter 3.1.1, an UWB signal has a huge amount of advantages, for instance its *High efficiency against Multi-Path,* so that the information can be received in a very short time and the LoS signal is likely to be not disturbed by the others, which can be isolated. Hence, from the impulse response we could obtain the Power Delay Profile, which is very useful for a lot of applications.

Furthermore, it was interesting to study the same rich-of-scattering environment with other frequencies which are higher than the standard ones, but lower than the mmWave-signals frequencies.

Unfortunately, we had no enough time to make a complete Power Delay Profile, but with all collected data we managed to extract some Impulse Response in two different situation.

- Both Receiver and Transmitter stationary in a LoS condition (*Tx1_Rx5*).
- Receiver stationary (*Rx6*) and Transmitter on the drone (T*x6*) which was hovering at a specific height in a specific point (*Fig. 5.m*).

Positions of transmitters are not changed (same as the mmWave measurement setup), receivers Rx5 and Rx6 positions are shown in *Fig. 5.n.*

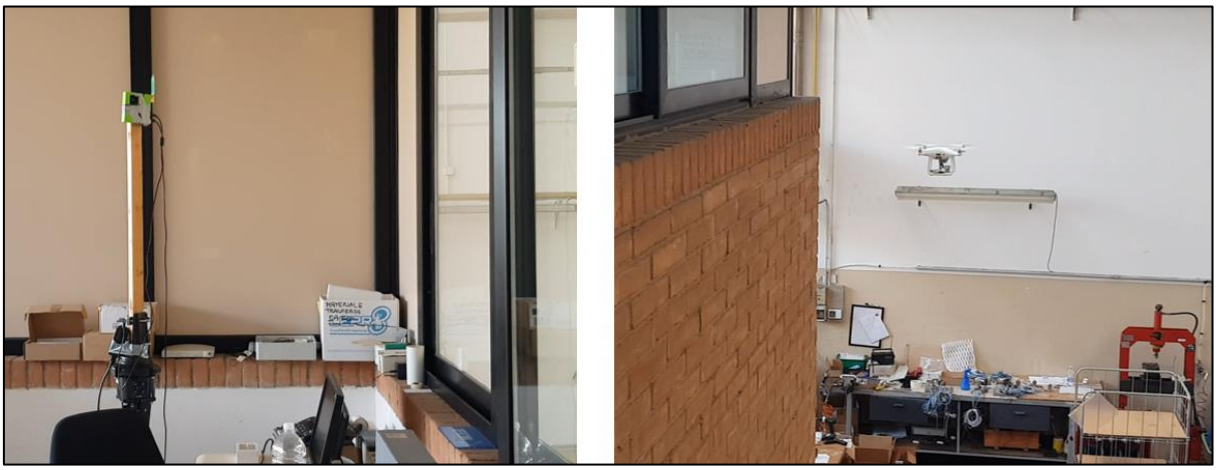

Figure 5.m On the Left the UWB fixed in Rx6 in Gianni's office as a receiver, on the right the drone in Tx6 as a transmitter.

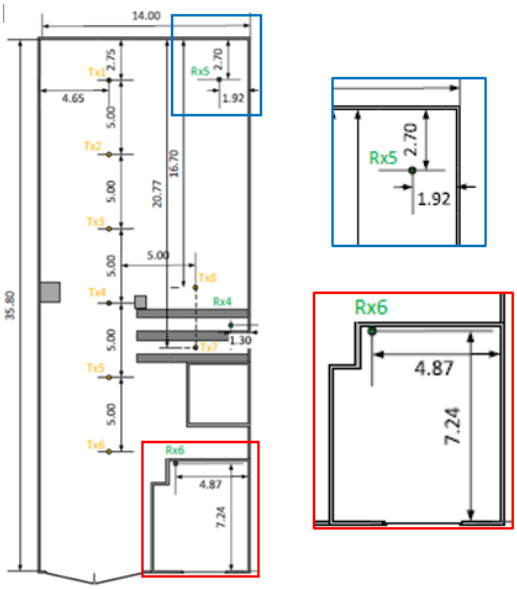

Figure 5.n Positions on the map.

5.3.2. Equipment for the experiment.

The equipment for this experiment was:

- Two P410s of the Time Domain used as Ranging Radios. Basically, they all have the same function: sending UWB signals with the omnidirectional antennas.
- A drone. We used a "DJI Drone Phantom 4", but any quadcopter is good since it can lift at least 70 grams (weight of the P410 plus the plastic support) and it is stable enough. (*Fig 5.o*)

- One omnidirectional antenna (the blue one) connected to the P410 on the drone, with *gain* = 3 dBi, used as a transmitter.
- One omnidirectional antenna (the green one) which is stationary, with *gain* = 3 dBi, used as a receiver *(Fig. 5.p*)
- A support to mount the P410 under the drone. We had to 3D-print it in order to lift the weight efficiently and avoid imbalances.
- A 9 V battery to power the P410.
- Two tripods for Rx and Tx (in the situation without drone).

Figure 5.o The DJI Phantom we used for the experiment. Below it there was the 3D-printed support for the P410.

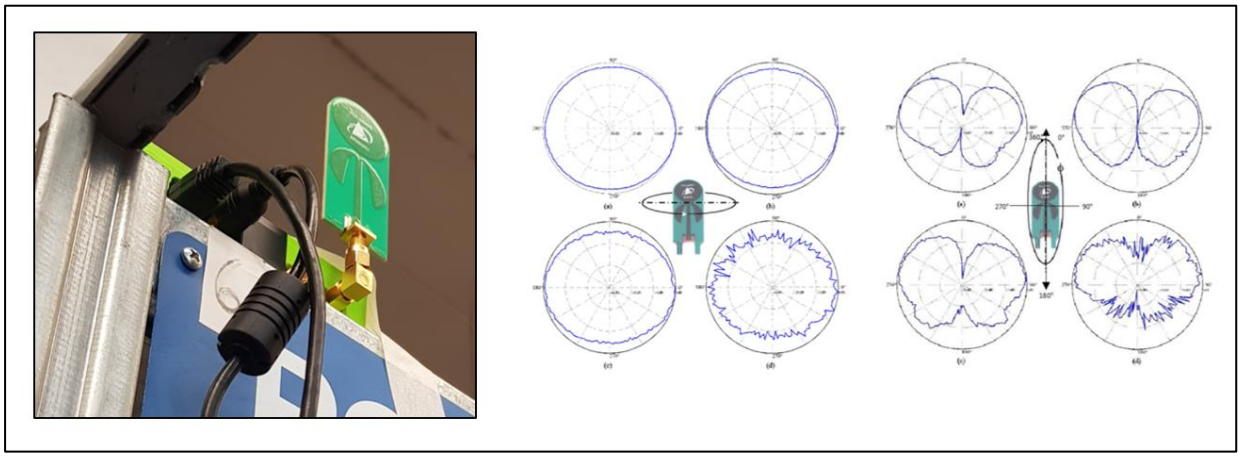

Figure 5.p On the left the receiver antenna fixed at one position, on the right the azimuthal and elevation beam pattern

5.3.2. The Impulse Response.

From theory we know that the Impulse Response is the output when presented a brief input signal (for instance a Dirac Delta), or in other words it is the reaction of any dynamic system in response to some external change, as a function of time.

So, if the signal (*x*) passes through a linear and time-invariant system, the response (*y*) will be the convolution of the signal and the Impulse Response:

$$y(t) = x(t) * h(t)$$

But to obtain the *h(t)* we need first, to switch to the frequency domain:

$$Y(f) = X(f)H(f)$$

$$H(f) = \frac{Y(f)}{X(f)}$$

And then, with an Inverse Fourier Transform we can extract the *h(t).*

With the Impulse Response other functions could be performed, such as the Power Delay Profile (PDP) or the Power Angle Delay Profile, both fundamental in any propagation researches.

Here, for reasons of time, only the Impulse Response will be analysed.

So, speaking of the experiment, the UWB transmits a "Gaussian Monocycle Impulse" (*Fig. 5.o*), that basically replaces the Dirac Delta of theory.

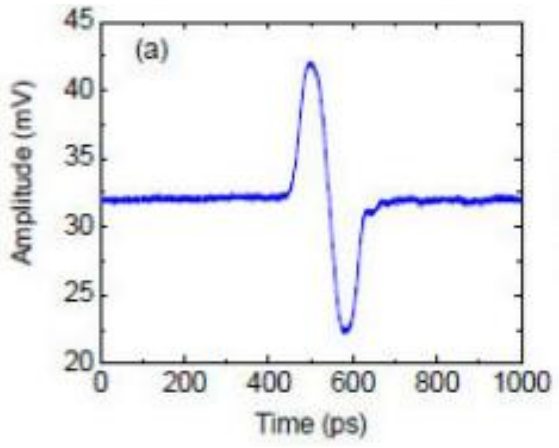

Figure 5.o The Gaussian Monocycle, the input pulse for UWB systems

Then we basically put the ".csv" files from the measurements and process them with Matlab.

5.3.3. Results and Conclusions.

If we imagined Transmitter and Receiver as connected with a long ideal wire (without the environment medium), the response would be as shown in *Fig. 5.p.*

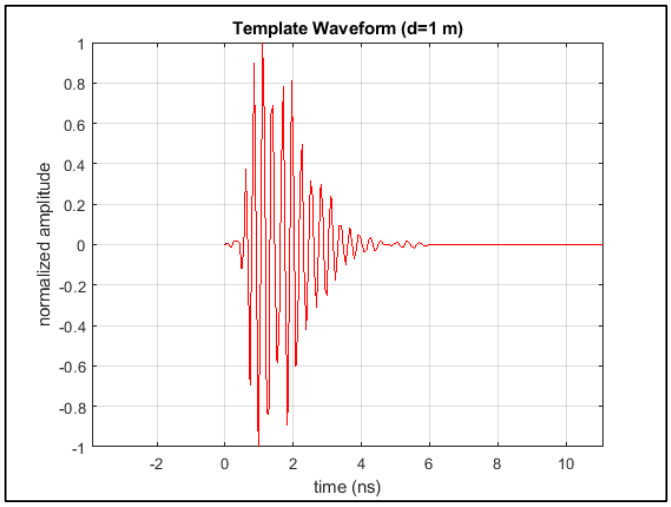

Figure 5.p Template Waveform considering only the non-ideal Time Domain equipment

From the consideration of the propagation in the environment we will have the received signal (the first plot in the following figures) and the Impulse Response, which basically is the deconvolution of the received signal and the Template Waveform.

For our experiment, two different cases of interest are considered:

- *Tx1_Rx5*: both stationary in a LoS condition. In this case what we expect from the Impulse Response is a standard situation where there is a principal peak, which is also the first one (the first to be received is also the LoS one, so stronger), and then other minor peaks. See *Fig. 5.q*

  In this simple case a mathematical proof of what we see can also be done.

In fact, the first peak is the LoS one, hence, knowing distance (about 6.5 m) and the speed of light ($3*10^8$), the time coincides to the position of that peak in time (about 21.8 ns).

- *Tx6_Rx6:* Here the situation is not standard anymore and it is a NLoS condition. We expect many peaks and the first ones are not necessarily the strongest. Moreover, the vibration of the drone influences the propagation of the signal and many MPCs could arise. See *Fig. 5.r*

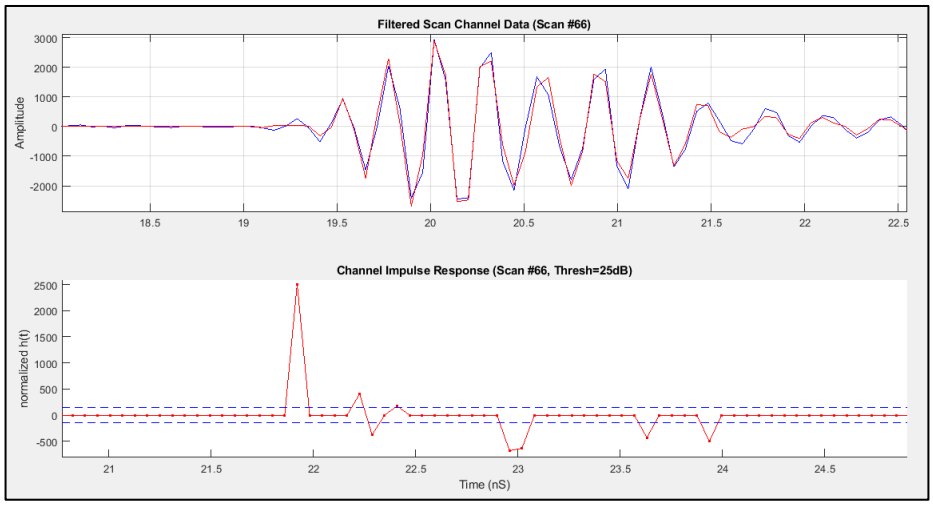

Figure 5.q Received signal and Impulse Response of Tx1_Rx5 in Los condition.

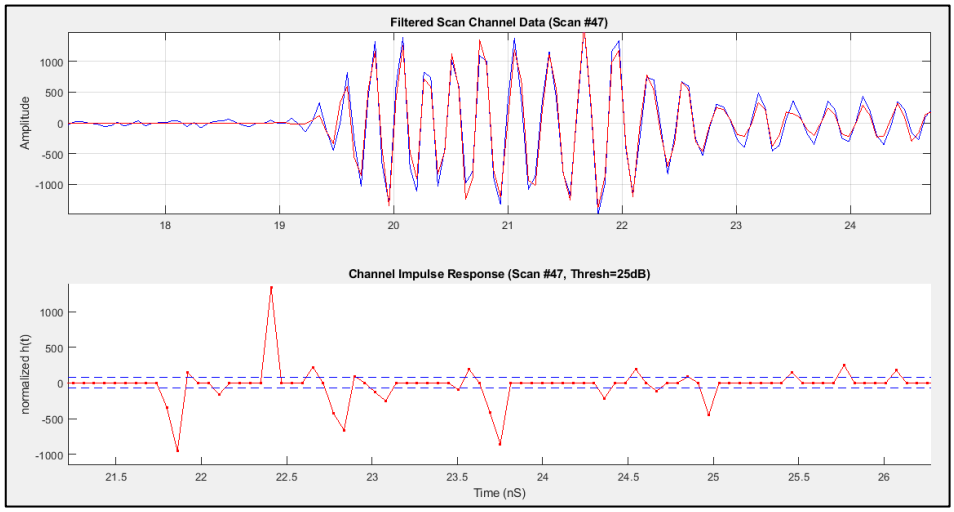

Figure 5.r Received signal and Impulse Response of Tx6_Rx6 with drone and NLoS condition.

CHAPTER 6

MEASUREMENT CAMPAIGN IN URBAN ENVIRONMENT

6.1 Introduction.

6.1.1. Description and Channel Plan of Measurement.

Unfortunately for reason of time, only the plan of measurement will be here presented, but results will be available soon.

Anyway, the Measurement Campaign can be divided into three different experiments, which will be organized in three different parts of the city:

- in the historical center of Imola (Via Callegherie), to study the propagation of signal in a typical urban environment, with UWB and mmWave setup measurement;
- in a suburban environment (Via Petrarca) with the same setup measurements;
- the last one in a green area (close to Via Tabanelli) using the same setup we used in factory environment.

Measurement at UWB frequencies will be done in a range from 3.1 – 5.3 GHz and for mmWave frequencies we will use 27 GHz and 38 GHz.

For each street, the drone will be placed on a vertical plane orthogonal to the street and on a horizontal plane along the street.

There will five discrete positions at different heights (with multiple orientations with the directive antenna to measure the Power Angle Profile) and there will be four continuous trajectories (both vertical and horizontal) in order to analyse a dynamic situation.

On the vertical plane, two different setup measurement will be done:

- With the terrestrial terminal in (x_{a1}, y_{a1}) and the drone in all positions and trajectories.
- With the terrestrial terminal in (x_{a2}, y_{a2}) and just the continuous trajectories.

On the horizontal plane, measurements will be done with the terminal on the ground in (x_{a1}, y_{a1}) or in (x_{a2}, y_{a2}). Positioning schemes in *Figg. 6.a and 6.b.*

In the green open area the idea is to deploy the drone hovering on discrete points, with the directive antenna towards a determined target (a house or a tree) in order to measure scattering radiations at 27 and 38 GHz or Power Angle Profiles with different orientation of the antenna.

The height h_T of the terrestrial station is always 2 m. except where it is indicated.

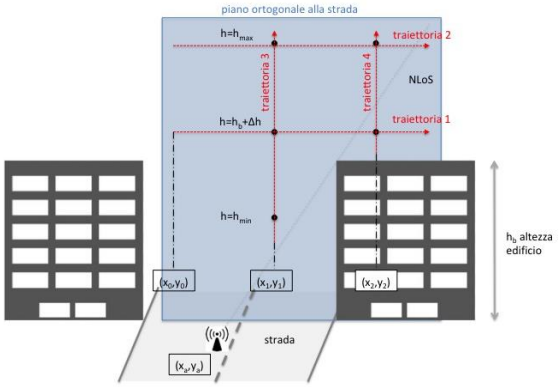

Figure 6.a Measurement on the vertical plane, orthogonal to the street.

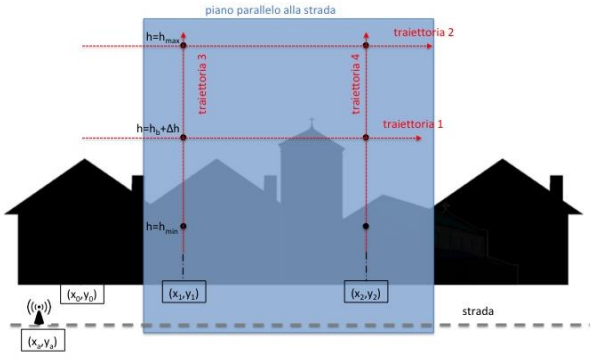

Figure 6.b Measurement on the horizontal plane, along the street.

6.1.2. Example of a sequence of measurement in a street.

As already said there will be two plans in which we will do measurements.

For the Vertical plane the sequence could be:

- The Terrestrial Terminal (Tx at mmWave and Rx + PC at UWB) in (x_{a1}, y_{a1}).
- Drone with directive antenna on six different points and multiple (24) angular orientations for 2 h, then we need to change battery of the drone.
- Drone with omnidirectional antenna on the four trajectories for 45 min. Then we move the Terrestrial Terminal.
- Terrestrial Terminal in (x_{a2}, y_{a2}).
- Drone with omnidirectional antenna on the same 4 trajectories for 45 min.

For the Horizontal plane the sequence could be:

- Terrestrial Terminal (Tx at mmWave and Rx + PC at UWB) in (x_{a1},y_{a1});
- Drone with directive antenna on discrete points a multiple angular orientaions for 2 h, then we need to change battery of the drone;
- Drone with omnidirectional antenna on the 4 trajectories for 45 min.

Estimated total time: 6 h and 15 min, excluded set up time and lunch break.

6.2 Experiment in Via Callegherie.

6.2.1. Plan of measurement and Positioning Parameters.

The map of the area with positioning for both plans in *Fig. 6.c.* Parameters for both the planes and positions are explained below.

With Δh = 3m; $hmax$ = 50m.

For the Vertical Plane:

- *xa1, ya1 =* 44.354889°, 11.716902°
- *xa2, ya2 =* 44.354381°, 11.718167°

- *x1, y1 =* 44.354846°, 11.717024°
- *x0, y0 =* 44.354804°, 11.717002°
- *x2, y2 =* 44.354906°, 11.717064°
- *1st Trajectory horizontal:* from (x0, y0, hb+Δh) to (x2, y2, hb+Δh)
- *2nd Trajectory horizontal*: from (x0, y0,hmax) to (x2, y2,hmax)
- *3rd Trajectory vertical*: from (x1, y1, hmin) to (x1, y1, hmax)
- *4th Trajectory vertical*: from (x2, y2, hb+Δh) to (x2, y2, hmax)

For the Horizontal Plane:

Tx in (x_{a2}, y_{a2}) and x0, y0 = x_{a2}, $y_{a2;}$

- *x2, y2 =* 44.355267°, 11.715969°
- *x1,y1 =* 44.354846°, 11.717024°
- *1st Trajectory horizontal*: da (x0, y0, hb+Δh) a (x2, y2, hb+Δh)
- *2nd Trajectory horizontal*: da (x0, y0, hmax) a (x2, y2, hmax)
- *2nd Trajectory vertical*: da (x1, y1, hmin) a (x1, y1, hmax)
- *3rd Trajectory vertical*: da (x2, y2, hmin) a (x2, y2, hmax)

Figure 6.c Via Callegherie with Positioning for measurements

6.3 Experiment in Via Petrarca.

6.3.1. Plan of measurement and Positioning Parameters.

The map of the area with positioning for both plans in *Fig. 6.d.* Parameters for both the planes and positions are explained below.

With Δh = 3m; *hmax* = 50m.

For the Vertical Plane:

- *xa1, ya1 =* 44.347022°, 11.714008°
- *xa2, ya2 =* 44.347825°, 11.714003°
- *x1, y1 =* 44.346925°, 11.714008°
- *x2, y2 =* 44.346919°, 11.713819°
- *1st Trajectory horizontal*: from (x1, y1, hb+Δh) to (44.346925°, 11.713750°, hb+Δh)
- *2nd Trajectory horizontal*: from (x1, y1, hmax) to (44.346925°, 11.713750°, hmax)
- *3rd Trajectory vertical*: from (x1, y1, hmin) to (x1, y1, hmax)
- *4th Trajectory vertical*: from (x2, y2, hb+Δh) to (x2, y2, hmax)

For the Horizontal Plane:

Tx in (xa1, ya1) and x0,y0 = xa1,ya1;

- *x1, y1 =* 44.347825°, 11.714003° (= xa2, ya2)
- *x2, y2 =* 44.348739°, 11.714008°
- *1st Trajectory horizontal*: from (x0, y0, hb+Δh) to (x2, y2, hb+Δh)
- *2nd Trajectory horizontal*: from (x0, y0, hmax) to (x2, y2, hmax)
- *2nd Trajectory vertical*: from (x1, y1, hmin) to (x1, y1, hmax)
- *3rd Trajectory vertical*: from (x2, y2, hmin) to (x2, y2, hmax)

Figure 6.d Via Petrarca with Positioning for measurement

6.4 Experiment in a Green Area close to Via Tabanelli.

6.4.1. Plan of measurement and Positioning Parameters.

In the Green Area measurement will be done on three different points and two trajectories. Then the idea is to do some scattering measurements (at 27 GHz and 38 GHz) from two different buildings and on six-teen different points placed on arcs of circles at 15° angular distance.

The directive antenna on the drone will point towards the center of the spot enlightened by Tx, indicated with “Center of Circles”.

In *Fig. 6.e* there is the map of Via Tabanelli and in *Fig 6.f* a scheme of scattering measurement is shown.

Parameters and Positions for the Green Area:

- xa1, ya1 = 44.348678°, 11.718728°
- x1, y1 = 44.348008°, 11.716689°
- traiettoria 1 orizzontale: da (x1,y1) a (44.348008°, 11.717956°)
- traiettoria 2 verticale: da (x1,y1, hmin) a (x1,y1, hmax)

Scattering Measurement of the building with balcony:

- hT = 4.5m
- xa2, ya2 = 44.347728°, 11.715419°;
- Center of circles = (44.347739°, 11.715240°, h = hT),
- Circle Radius = 12m

Coordinates on the horizontal semicircle:

Lat	Lon	h
44.3477473537102	11.7152537256604	4.5 (=h_T)
44.3477725666982	11.7152912715666	“
44.3477951720336	11.7153249343326	“
44.3478136292048	11.7153524198850	“
44.3478266803914	11.7153718551159	“
44.3478334361813	11.7153819155351	“
44.3478334361813	11.7153819155351	“
44.3478266803914	11.7153718551159	“
44.3478136292048	11.7153524198850	“
44.3477951720336	11.7153249343326	“
44.3477725666982	11.7152912715666	“

Coordinates on the vertical quarter of circle:

Lat	Lon	h
44.347725	11.7152355234562	5.50
“	11.7152452610328	8.40
“	11.7152640725858	11.00
“	11.7152906761385	13.12
“	11.7153232587021	14.62
“	11.7153595998280	15,40

Scattering Measurement of the building without balcony:

- xa3, ya3 = 44.347447°, 11.715388°; hT = 4.5m
- Center of Circles = (44.3474416°, 11.715225°, h = hT),
- Radius of circle = 12m

Coordinates on the horizontal semicircle:

Lat	Lon	h
44.3474508594988	11.7152533928096	4.5 (=h_T)
44.3474771687097	11.7152925709429	“
44.3475007568906	11.7153276971261	“
44.3475200165511	11.7153563775554	“
44.3475336351829	11.7153766576928	“
44.3475406847039	11.7153871554681	“
44.3475406847039	11.7153871554681	“
44.3475336351829	11.7153766576928	“
44.3475200165511	11.7153563775554	“
44.3475007568906	11.7153276971261	“
44.3474771687097	11.7152925709429	“

Coordinates on the vertical quarter of circle:

Lat	Lon	h
44.34744166	11.7152343993047	5.56
“	11.7152445602028	8.59
“	11.7152641895503	11.30
“	11.7152919496390	13.52
“	11.7153259486639	15.08
“	11.7153638696471	15.89

Figure 6.e Via Tabanelli and Positions for measurements

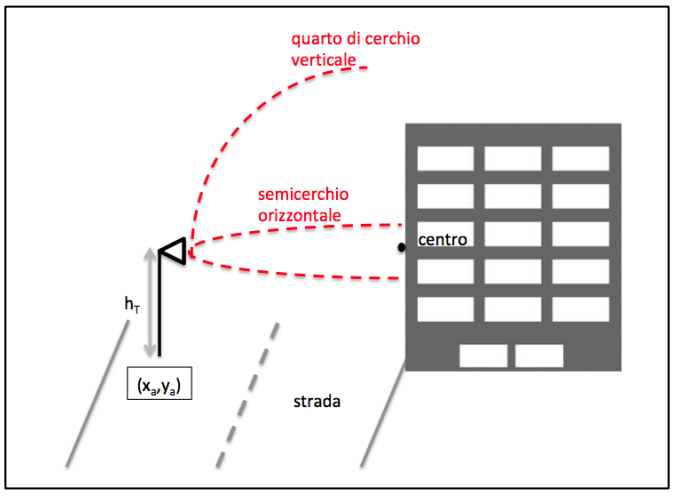

Figure 6.f Scheme for Scattering Measurements from building

CONCLUSIONS

Given the worldwide need for cellular spectrum, and the relatively limited amount of research done on mmWave and UWB communications in a rich-scattering environment, we have conducted a measurement campaign in a factory scenario and planned another one in an urban scenario.

This work presents data collected during the campaign in the factory in Pontecchio and the plan of measurements in Imola whose results will be available soon.

Basically, the aim was to put into practice what we already know about physics behind the behavior of signals and their propagation in interesting scenarios at different frequencies. In this specific case, the propagation was in a factory, where obviously signals are likely to be subjected to a large amount of reflections and diffractions. Then, we split the campaign into two different experiments: the mmWave Measurement Setup (at 27 or 38 GHz) to get the "Power Angle Profile" and the Ultra-Wide Band Measurement Setup (center frequency at 4.3 GHz) with the drone to get the "Impulse Response", both incredibly helpful functions for propagation at high frequencies.

Speaking of results, we found that the polar pattern of PAPs is quite easy: a principal lobe in LoS condition and a pair of size lobes for the main reflections. Similarly, we also observed that the impulse response does not have a difficult plot, but only few peaks in time. It means that many researches could be done to perform, for instance, directive antenna arrays or directional beamforming, which basically can exploit the main paths of the signal propagation in a dynamic way.

To sum up, this experience taught us that mmWave signals could work, even in complex environment and could be a fundamental part for the development of

future cellular communications. The UWB signals, instead, confirmed their enormous potential in indoor positioning and, for LoS condition, even a quite standard Impulse Response.

So yes, maybe we are still starting out and several researches should still be done, but overall “Progress” begins with small steps…

REFERENCES

[1] T. Tozer and D. Grace, "High-altitude platforms for wireless communications", *Electronics & Communication Engineering Journal,* vol. 13, no. 3, pp.127-137, 2001.

[2] S. Rohde and C. Wietfeld, "Interference Aware Positioning of Aerial Relays for Cell Overload and Outage Compensation", in *IEEE Vehicular Technology Conference (VTC Fall),* 2012, pp 1-5.

[3] "Characteristics of unmanned aircraft systems and spectrum requirements to support their safe operation in non-segregated airspace", Int. Telecommunication Union, Geneva, Switzerland, ITU-R M.2171, Dec. 2009.

[4] "Unmanned Aircraft Systems (UAS) Service Demand 2015-2035: Literature review and projections of future usage", US Dept. of transp., Washington, DC, USA, Tech. Rep., v.1.0, DOT-VNTSC-DoD-13-01, Feb. 2014.

[5] A. Osseiran et al., "Scenarios for 5G Mobile and Wireless Communications: the Vision of the METIS Project", IEEE Commun. Mag., vol.52, no. 5, May 2014, pp. 26-35.

[6] Yong Zeng, Rui Zhang and Teng Joon Lim, "Wireless Communications with Unmanned Aerial Vehicles: Opportunities and Challenges", IEEE Communications Magazine, May 2016.

[7] A. Merwaday and I. Guvenc, "UAV assisted heterogeneous networks for public safety communications", in *Proc. of IEEE Wireless Communications and Networking Conference Workshops (WCNCW),* March 2015.

[8] Dmitrii Solomitckii, Margarita Gapeyenko, Vasilii Semkin, Sergey Andreev, and Yevgeni Koucheryavy, "Technologies for Efficient Amateur

Drone Detection in 5G Millimiter-Wave Cellular Infrastructure", IEEE Communications Magazine, Jan., 2018.

[9] D. W. Matolak, "Air to Ground channels and models: comprehensive review and considerations for unmanned aircraft systems", in *Proc. IEEE Aerospace Conf.*, Big Sky, MT, Mar. 3-10, 2012, pp. 1-17.

[10] International Telecommunications Union (ITU), "Propagation curves for aeronautical mobile and radionavigation services using the VHF, UHF, and SHF bands", Rec. ITU-R P.528-2, 1986.

[11] J. Karedal, F. Tufvesson, N. Czink, A. Paier, C. Dumard, T. Zemen, C. F. Mecklenbrauker, and A. F. Molisch, "A geometry-based stochastic MIMO model for vehicle-to-vehicle communications," IEEE Trans. Wireless Commun., vol. 8, no. 7, pp. 3646–3657, July 2009.

[12] D. W. Matolak, "AG channel measurements and modeling: Initial analysis and flight test planning", NASA Glenn Research Center, Grant NNX12AD53G, Tech. Rep. 2, June 8, 2012.

[13] A. F. Molisch, H. Asplund, R. Heddergott, M. Steinbauer, and T. Zwick, "The COST259 directional channel model-part I: Overview and methodology", IEEE Trans. Wireless Commun., vol. 5, no. 12, pp. 3421-3433, Dec. 2006.

[14] David W. Matolak, and Ruoyu Sun, "Air-Ground Channel Characterization for Unmanned Aircraft Systems-Part I: Methods, Measurement, and Models for Over-Water Settings, IEEE Transactions on Vehicular Technology, vol. 66, no. 1, Jan. 2017.

[15] H. L. Bertoni, "Radio Propagation for Modern Wireless Systems", Prentice Hall, Pearson 2001.

[16] A. Al-Hourani, S. Kandeepan, and A. Jamalipour, “Modeling air-toground path loss for low altitude platforms in urban environments,” in Proc. GLOBECOM Symp. Sel. Areas Commun., Satellite Space Commun., Austin, TX, USA, Dec. 2014, to be published.

[17] Q. Feng, J. McGeehan, E. Tameh, and A. Nix, “Path loss models for air-toground radio channels in urban environments,” in Proc. IEEE 63rd VTCSpring, May 2006, vol. 6, pp. 2901–2905.

[18] “Propagation data and prediction methods for the design of terrestrial broadband millimetric radio access systems,” Geneva, Switzerland, Rec. P.1410-2, 2003, P Series, Radiowave Propagation.

[19] A. Al-Hourani, S. Kandeepan, and Simon Lardner, “Optimal LAL Altitude for Maximum Coverage, IEEE Wireless Communications Letters, vol. 3, no. 6, Dec. 2014.

[20] A. Al-Hourani, S. Kandeepan, and Abbas Jamalipour, “Modeling Air-to-Ground Path Loss for Low Altitude Platforms in Urban Environments”, Globecom 2014.

[21] S. Rohde and C. Wietfeld, “Interference Aware Positioning of Aerial Relays for Cell Overload and Outage Compensation,” in IEEE Vehicular Technology Conference (VTC Fall), 2012, pp. 1–5.

[22] T. Tozer and D. Grace, “High-altitude platforms for wireless communications,” Electronics & Communication Engineering Journal, vol. 13, no. 3, pp. 127–137, 2001.

[23] Win, Moe Z., and Robert A. Scholtz. "Ultra-wide bandwidth time-hopping spread-spectrum impulse radio for wireless multiple-access communications." IEEE Transactions on communications 48.4 (2000): 679-689.

[24] Z. Pi and F. Khan, "An introduction to millimeter-wave mobile broadband systems", *IEEE Comm. Magazine*, Vol. 49, No. 6, pp. 101-107, Jun. 2011.

[25] Federico Boccardi, Bell Labs, Alcatel-Lucent, Robert W. Health Jr., The University of Texas at Austin, Angel Lozano, Universitat Pompeu Fabra, Thomas L. Marzetta, Bell Labs, Alcatel-Lucent, Petar Popovski, Aalborg University, "Five Disruptive Technology Directions for 5G".